RSC Advances

REVIEW

View Article Online
View Journal | View Issue

Cite this: *RSC Adv.*, 2025, **15**, 12382

Atomic layer deposition on flexible polymeric materials for lithium-ion batteries

Edy Riyanto

Polymers have the distinctive qualities of being lightweight, flexible, and inexpensive and possessing good mechanical qualities. Consequently, these materials are employed in a wide range of applications, including lithium-ion batteries (LiBs). Interestingly, a variety of thin film materials can be deposited onto polymer substrates using the atomic layer deposition (ALD) technique. This is because the surface of many polymers has abundant reactive sites that are essential for the initial growth of ALD, such as functional hydroxyl –OH groups and –C=O polar groups, aiding the smooth growth of ALD materials. Moreover, the diffusion growth mechanism, which is initiated by the nucleation and infiltration of precursors, can enable the initial growth of ALD materials even if the polymers lack these reactive polar groups. As polymers are composed of several chains, they have microporous characteristics, forming voids between the polymer chains. Because of these characteristics, polymers are considered ideal material substrates for investigating the promising future of the widely used ALD technique. The combination of polymer materials and the ALD method is becoming increasingly important in the advancements of high-performance LiBs. This review focuses on the present understanding of the role of polymer materials in the ALD technique for the fabrication of lithium-ion batteries.

Received 27th January 2025
Accepted 2nd April 2025

DOI: 10.1039/d5ra00652j

rsc.li/rsc-advances

Research Center for Advanced Material, National Research and Innovation Agency, Serpong, 15314, Indonesia. E-mail: edy.riyanto@brin.go.id

Edy Riyanto

Dr Eng. Edy Riyanto received his Bachelor's degree (2006) in Mechanical Engineering from Gadjah Mada University (Indonesia). He has worked as an Assistant Researcher at the Indonesian Institute of Sciences (2008–2010), which is now known as the National Research and Innovation Agency. Subsequently, he earned his Master's degree (2013) in Materials Science and his PhD (2017) in Material Physics and Chemistry from Donghua University (China). From March 2014 to March 2017, he was a Visiting Research Student at Fudan University's Department of Materials Science (China), where he worked on his PhD thesis. Both his Master and PhD theses were related to atomic layer deposition. After completing his Doctoral study, he joined the Research Center for Electrical Power & Mechatronics, National Research and Innovation Agency (April 2018–March 2022). Presently, his surface engineering research is focused on atomic layer deposition. He has published 10 articles on the subject of atomic layer deposition, six of which are SCI articles. He is currently a Senior Researcher at the National Research and Innovation Agency's Research Center for Advanced Materials (March 2022 to present).

Introduction

Atomic layer deposition (ALD) is a very effective technique for creating uniform films and dense coatings with a controllable thickness at the nano, Angstrom, and atomic levels. It can produce complex nanostructured materials, including core–shell nanomaterials, nanotubes, porous nanomaterials, and nanospheres, regardless of their complex geometric shapes.[1–4] Conformal nanoscale metal coatings on polymer materials can be achieved using the sophisticated technique of atomic layer deposition.[5–7] Owing to its conformal deposition, ALD can deposit materials onto 3D substrates uniformly and produce thin film materials with a single layer as thin as 0.1 nm. ALD-coated polymers can serve as a solid foundation for a wide range of technical uses. Sophisticated filtering, reinforced composites, flexible electronics, and sensors are a few of the new applications enabled by using natural and man-made polymeric materials in ALD processes,[6,8–10] together with energy applications and organic light-emitting diode devices (OLEDs),[11–13] catalysis,[14,15] and dental materials made of polymers.[16] Because of their loose molecular structure and numerous internal pores, which result in a high water vapour permeability in the corresponding encapsulated films, the common organic thin film materials, such as polyethylene terephthalate (PET) and polyimide (PI), cannot meet the requirements of OLEDs.[17,18] Alternatively, room-temperature barrier coating of aluminium oxide (Al_2O_3) can significantly enhance the capacity of OLEDs to fend off water vapour and prevent serious damage to OLEDs during deposition.[17,19]

Polymers are usually effective for creating oxide spheres, nanotubes, and other shapes, when used as sacrificial nanostructured templates.[12,20,21] When the ALD coating creates a good conformal layer, the polymer dissolves and leaves behind an inorganic shell, which resembles the outside of the 3D template. After exposure to the reactants, a calcination step can produce a solid three-dimensional structure when the precursor has significantly diffused into the polymer.[12,22] ALD is considered one of the technologies with the greatest potential for thin-film deposition in applications related to renewable energy (*e.g.*, lithium-ion batteries (LiBs) and solar cells).

Currently, energy supplies still depend on fossil fuels, such as coal, oil, and natural gas, which are finite resources and contribute to environmental problems. Thus, it is essential to replace these energy sources with alternative renewable energy sources (*e.g.*, solar radiation and wind) to guarantee sustainable future development. However, although these sources are thought to be limitless and eco-friendly, the energy they produce is sporadic because of changes in the weather and the sun's location. Thus, to address this issue, electrical energy storage systems are required, and at present, LiBs are considered the most encouraging electrochemical devices. In the present era, the necessity for clean energy in large quantities is not the only factor driving battery research and development. Another factor is the rise in portable devices with special features, such as wearable smart textile power supplies and flexible electronic devices. Thus, the use of ALD procedures and polymeric materials for the fabrication of energy storage devices is growing to provide dependable power sources that can sustain these diverse contemporary electronic devices.

Energy storage for powering smart portable electronic devices, flexible electronics (such as flexible solar cells, supercapacitors, and sensors), smart wearable textiles, which are related to the electronic-textile segment, and materials used in clinical implants, improving the ability of polymer materials to be biocompatible, are a few of the futuristic technologies that can use atomic layer deposition material-coated polymer materials. Notwithstanding the fact that scholars have examined the function of ALD in lithium-ion batteries, as reported by Peng *et al.*,[4] Meng *et al.*,[23–25] and Edy *et al.*,[26] a review on the use of polymers in the ALD process for improving the performance of LiBs is still lacking to date. It is important to note that the ALD process can be employed to deposit many different materials in complex structures, including polymeric microporous structures, to obtain highly uniform and conformal coatings, and thus it has great potential to be applied for accelerating battery development to support the next generation of smart technologies. Alternatively, the involvement of polymer materials in the present trend of smart wearable electronics is inevitable. All these devices need to be powered by energy storage on a platform that is lightweight, flexible, inexpensive, and environmentally friendly. However, the combination of ALD materials and polymers is mainly still used only for the separator component in lithium-ion batteries. The newest developments in ALD, which use polymers as the substrate (natural and synthetic), as well as its growth process and use in LiBs are discussed in this study. This review article focuses on the ALD process employing polymers as the substrates, and subsequently employed in LiBs. The aim of this review is to summarise the use of ALD on polymer substrates and its applications in lithium-ion batteries, which is distinct compared to earlier review papers on the subject of ALD for use in lithium-ion batteries.

Basic principle of ALD process

ALD is a deposition method that creates ultrathin conformal films at a controlled pace by means of a sequence of surface-saturated, self-limiting reactions. In particular, ALD is the only approach that enables the accurate control of the thickness on the angstrom scale during the deposition of 2D conformal nanofilms and related wafer-scale heterostructures, with excellent step coverage and no defects.[27–31] The precise deposition of homogenous and conformal thin films at the intricate curves of the underlying substrate structures is crucial in numerous technologies. Atomic layer deposition is a method that can provide these thin film characteristics. ALD occurs *via* layer-by-layer growth mechanisms to create a layer, which is carried out by a series of alternating, self-terminating surface reactions. One of the most crucial concerns in ALD growth is the so-called ALD window, as shown in Fig. 1. The range of temperatures in which film growth exhibits an ALD window is identified to show self-limiting ALD growth behavior.[32,33] The rate of the formation of films within the ALD window process appears to be roughly constant. However, it should be mentioned that occasionally, the growth rate may exhibit significant temperature variations while maintaining the self-limiting behavior.[32,34] Each precursor undergoes two self-limiting half-reactions to be chemically adsorbed, creating each ALD layer. In contrast to alternative deposition methods (*i.e.*, chemical vapor deposition and sputtering), ALD has several advantages. The chemical process stops when the surface adsorption sites are saturated with a particular type of precursor molecule, exhibiting self-limiting growth behavior.[35–39] Furthermore, to increase the activity of the ligand-exchange processes, the quantity of hydroxyl (–OH) groups on the outermost layer is essential.[2,40] The purging phase occurs after each half-reaction during exposure to the precursor in the ALD reactor to guarantee the purity of the ideal ALD process.

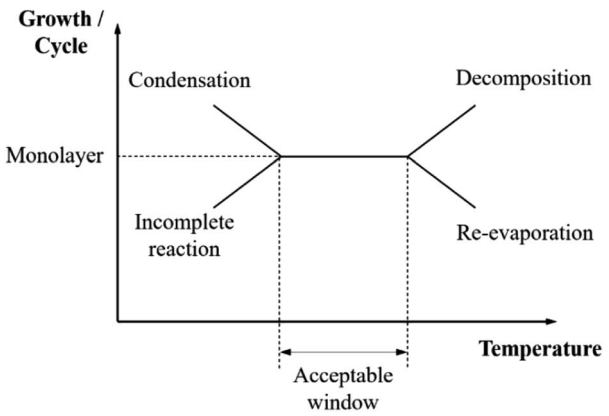

Fig. 1 Diagram of ALD characteristics as a function of temperature.

The purpose of this step is to remove the surplus precursor and reaction product.

The ALD development rate as a function of temperature is shown in Fig. 1, which also highlights a general ALD growth. The growth rate may increase as a result of precursor decomposition if the temperature used is higher than that required to produce a chemisorption reaction. This can disrupt the saturated chemisorption reaction.[26,41] The growth rate of each cycle can be increased by precipitation on the surface from precursor breakdown at high temperatures. Alternatively, re-evaporation of the topmost layer may cause a reduction in the number of surface groups, which can slow down growth at a higher temperature.[42] Because chemisorption is reduced at low deposition temperatures, reactant condensation results in the formation of many monolayers, therefore increasing the growth rate.[42] The growth rate falls at low temperatures because the chemical reaction requires sufficient activation energy to finish the surface reaction, which is impossible at low deposition temperatures.

The metal–ligand compound (ML_n) reaction and the water (H_2O) reaction, known as the ML_n/H_2O ALD process, are the two reactions that frequently repeat in cycles for metal oxides.[43] Assuming that ML_n reacts through "ligand exchange" with one or more (y) substrate hydroxyl (OH) groups, HL is released as a gaseous reaction product, and an ML_{n-y} species is attached to the surface (the surface is indicated by the symbol ||, and the gas phase is indicated by the symbol g).

$$y\|\text{–OH} + ML_{n(g)} \rightarrow (\|\text{–O–})_yML_{n-y} + yHL_{(g)} \quad (1)$$

More HL is released when H_2O reacts with the adsorbed ligands, substituting OH groups for them:

$$\|\text{–L} + H_2O_{(g)} \rightarrow \|\text{–OH} + HL_{(g)} \quad (2)$$

In the subsequent reaction cycle, the ML_n molecule and these OH groups interact once more. The ALD development of oxide materials is mediated by OH groups, according to this approach.

Film growth in the majority of thin-film deposition methods is dependent on the type and speed of precursor transport, in addition to the chemical reaction kinetics. Alternatively, a method for creating thin films is ALD, which is distinguished by film growth that occurs independently of transport and is accomplished by dividing the process into half-reactions that have reached saturation.[44,45] Given that it has been demonstrated to have high adhesion on a broad variety of substrates as well as chemical and thermal stability, Al_2O_3 is one of the most commonly utilised ALD coating materials and a typical example for the ALD process.[46–48] The common necessary precursors for the aluminium and oxygen sources are trimethylaluminum (TMA, $Al(CH_3)_3$) and deionized water (H_2O), respectively. Their reactions that result in the creation of an ALD Al_2O_3 layer on any substrate can be described as follows:

$$AlOH^* + Al(CH_3)_3 \rightarrow AlOAl(CH_3)_2 + CH_4$$

$$AlCH_3^* + H_2O \rightarrow AlOH^* + CH_4$$

where * indicates surface species. These reactions can be summarized as $2Al(CH_3)_3 + 3H_2O \rightarrow Al_2O_3 + 6CH_4$, which occur at a temperature as low as 35 °C.[49] The thermodynamic stability of Al_2O_3 and the strength of its Al–O and C–O bonds make it useful for improving the adherence of films to polymers.[50,51] To properly comprehend the entire ALD mechanism, several aspects must be considered, including non-covalent interactions between species, steric hindrance between ligands, availability of adsorption sites, and precursor exposure and purge duration.[52,53] Moreover, the reactor temperature is one of the most important parameters in the ALD deposition method. It must be set at the ALD window temperature to guarantee that the precursor and reactant can deposit onto the substrate precisely. To ensure that the self-saturated growth process and its associated advantages are not disrupted by the decomposition of the precursors, the precursors need to have thermal stability at the growth temperature.[54] Additionally, the usual ALD growth rate, or the thickness increment per cycle, rapidly increases until saturating, exhibiting self-limiting growth behavior. Although the hydroxyl concentration largely controls the saturation growth per cycle value, the bulkiness of the ligands also has a significant impact on the steric hindrance.[35,55] However, the film thickness attained in each cycle may be dependent on the dimensions of the precursor molecule given that steric hindrance among large precursors limits the amount of molecules that can adsorb on the surface.[28,56] Precursors with relatively tiny molecules allow full monolayer development in each cycle because the exposed precursors adhere to the adsorption sites on the surface *via* the ligand exchange reaction mechanism. In contrast to other methods (such as chemical vapor deposition (CVD), electron beam deposition, and pulsed laser deposition), ALD has a slow growth rate, making it a typical nano thin film technology. Given that the typical deposition rates are in the range of 100 to 300 nm per hour, growing micrometer-thick films *via* ALD is not feasible.[28] Also, the majority of thin film materials produced by ALD are in the amorphous state given that the process temperature is relatively low. Meanwhile, annealing at a high temperature is necessary in practical applications to transform or enhance these phases into a crystalline state.

Both physisorbed and chemisorbed incident precursor molecules can adhere to the substrate. The kinetics of a molecule determine whether it is desorbed off the surface, dispersed to another location, or trapped in the potential well. In the case of physisorption, the coverage progressively increases until it approaches the saturation value in the exposure step and falls back to zero during the purging phase. In the exposure step of chemisorption, the coverage progressively increases to 100% and remains constant during the purging phase. As shown in Fig. 2, both physisorption and chemisorption occur in a real ALD half cycle. To benefit from the self-terminating property of ALD, the optimal ALD process should have both saturate adsorption and full desorption of the physisorbed molecules. In the ALD reactor, usually a monolayer chemisorbed on a surface needs to have a greater binding energy than the layers that follow when the temperature is applied correctly.[26] The better

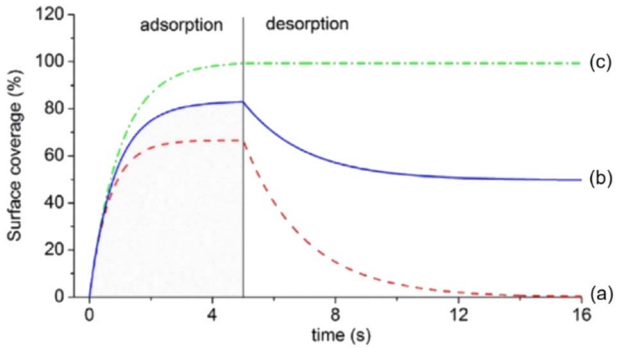

Fig. 2 Surface coverage during (a) physisorption, (b) actual ALD adsorption, and (c) chemisorption (reprinted with permission from ref. 57 copyright 2020 Elsevier B.V.).

the self-limiting mechanism of ALD, the larger the binding energy difference.

Characteristics of polymer materials

The synthetic polymers used most often on a daily basis include polypropylene (PP), polystyrene (PS), polyethylene terephthalate (PET), and polyethylene (PE), which are used in textiles, electronics, food packaging, and apparel. Their widespread use is mostly due to their highly valued physico-chemical characteristics, which include low cost, chemical inertness, mechanical strength, flexibility, and thermal resistivity.[58,59] Large molecules or macromolecules, made up of several subunits are called polymers. The structure that basically consists of the many repetition units is called a macromolecule. A polymer may be made up of linear macromolecules with a single unbranched chain or branched macromolecules (such as polyethylene).[60,61] In terms of structure, polymers are made up of several chains of polymers with microporous structures, while polymers with more regular repeated patterns (*i.e.*, semicrystalline or crystalline polymers) have a dense structure, and loose chain structure for amorphous polymers.

Li solid polymer electrolyte (Li-SPE) batteries are created by substituting a dry polymer electrolyte for the liquid electrolyte. The polymer electrolyte networks of entangled chains of a pure (dry) polymer facilitates the movement of Li ions. An electrolyte battery made of Li hybrid polymers (Li-HPE) was created shortly after this,[62,63] aiming to make use of the benefits of polymer electrolyte technology without the risks of Li metal.[64] Li-HPE is referred to as a "hybrid" given that it contains three different components, *i.e.*, a polymer matrix, a hybrid (gel) network made of a polymer that is semicrystalline with crystalline portions that improve the mechanical stability and amorphous sections that swell in a liquid electrolyte with a salt and a liquid solvent. A realistic Li-ion hybrid polymer electrolyte (HPE) battery that can be charged, known as an LiB made of plastic, is depicted in Fig. 3. This type of battery is very different from regular batteries, such as coin and cylinder batteries. With the ongoing trend towards electronic miniaturization, this battery technology using thin films, which provides a variety of forms, elasticity, and weightlessness, has numerous potential benefits. The synthetic concept of Li-ion is the basis for the next generation of Li-ion polymer batteries, which are anticipated to be employed in a variety of portable devices.

Because of their great potential for use in energy generation and medicine, polymer architectures have been widely studied. Polymers, which are made up of repeating monomer units, have unique properties such as flexibility, extensibility, and resistance to corrosion, making them ideal for a variety of uses, such as biosensors and medical equipment.[6] Depending on their origin, materials made of polymers can be separated into two groups, synthetic and natural polymers. Although synthetic polymers are fully man-made, natural polymers come from organic sources, which include a wide variety of animal and plant sources.[66] Materials based on polymers, including sheets, fibers, and textiles, have gained interest in a variety of uses due to their advantageous properties over other materials, such as metals and ceramics. Additionally, given technological and financial requirements, the comparatively large surface area, flexibility, light weight, and affordability of these materials make them beneficial.

In the context of the polymeric materials used in lithium-ion batteries through the ALD process, the merits of polymers such as their low cost, chemical inertness, mechanical flexibility, and weightlessness can be advantageous in the endeavor to enhance the battery functionality to support the storage of energy from different sources for powering the next generation of smart devices. Moreover, these materials, which are typically prone to degradation at high temperatures, are compatible with the typical ALD method, which permits the deposition of a wide variety of ALD materials at temperatures below 100 °C. These combinations of polymeric properties, the possibility of low deposition processes, and a variety of materials that can be deposited by ALD are great potential characteristics that can be used as capital to accelerate the development of lithium-ion batteries using polymers through the ALD process.

Vectran fabrics with and without ALD coating are shown in Fig. 4(a) and (b), respectively. Fig. 4(a) demonstrates that the fabric without coating is yellow, whereas Fig. 4(b) shows that the textile with a 1000 ALD cycle titanium dioxide (TiO_2) coating is white. The surface of the fabrics was enhanced by the TiO_2 nanocoating after 1000 cycles of deposition. The yellow Vectran

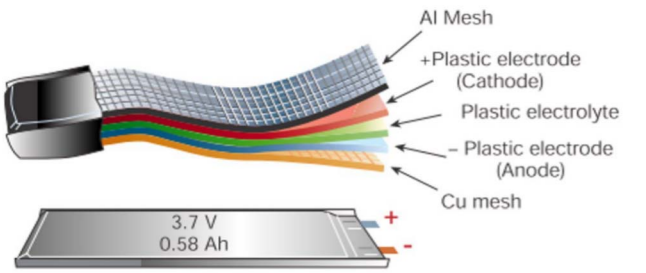

Fig. 3 Diagram displaying the components and form of different LiB designs. The thin and flat plastic Li-ion structure offers unique versatility; unlike the other configurations, it lacks free electrolyte (reprinted with permission from ref. 65 copyright 2021 Elsevier B.V.).

fabric turned white due to the buildup of a TiO_2 layer on the sample surface caused by these excessive deposition circles. The SEM images of the Vectran fiber prior to and following ALD are shown in Fig. 4(c) and (d), respectively. Fig. 4(c) demonstrates that the unmodified fiber had a diameter of around 50 μm with a smooth. In contrast, when ALD was used to coat the Vectran fiber with a thin layer of TiO_2 in 1000 cycles, it had an ultra-thin nanocoating and homogeneous exterior, which prevented any discernible deformation of the diameter of the fiber matrix (Fig. 4(d)). Additionally, perpendicular cracks were seen in the fiber coated with 1000 ALD cycles of TiO_2, indicating that the thickness of the TiO_2 film coated in 1000 ALD cycles was relatively rigid. This is consistent with our earlier research, which found that thicker TiO_2 nanosheets produced in 500–1000 ALD cycles are more rigid sheets, whereas those obtained in fewer ALD cycles had greater flexibility.[68] Despite being an amorphous phase, all the different thicknesses produced by the ALD process have different mechanical properties. It is because the atoms in the stiffer ALD film repeat more regularly than in the thinner ALD layer.[69–72] ALD-deposited TiO_2 on Vectran fibers is depicted in the high-magnification transmission electron microscopy (TEM) images in Fig. 4(e). With a thickness of about 389 nm, it was evident that the TiO_2 nanocoating produced in 1000 ALD cycles could adhere to the Vectran matrix consistently.

Fabrics or fibers combined with functional nanomaterials that can sense changes in their surroundings by enhancing one or more of their properties are known as smart textiles.[73,74]

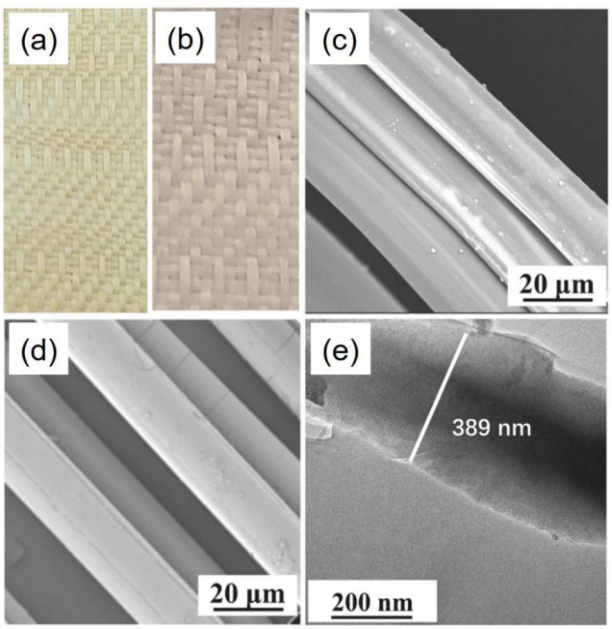

Fig. 4 ALD-modified Vectran textile colour variations with and without ALD coating. (a) 0 cycles and (b) 1000 cycles. SEM images of Vectran fibres under varying conditions: (c) Vectran fiber without modification and (d) Vectran fiber coated with ALD-1000 cycles. (e) TEM images of 1000 ALD cycles of TiO_2@Vectran fibre deposited using ALD (reprinted with permission from ref. 67 copyright 2023 Elsevier B.V.).

Excellent electrical, thermal, and electrochemical properties are provided by nanoparticle-encapsulating textiles, making them perfect substrates.[75,76] Because of their potential applications in training assessment, rehabilitation, and health monitoring, smart electronic textiles have attracted significant interest.[77,78] Smart textiles have been created using a variety of processes, where functional nanomaterials are integrated into polymer matrices, combined with a solvent and binder, and then supplied to an extrusion system.[75,79]

It was recognized that the most common methods for creating smart textiles including printing using conductive nanoparticle ink, dip coating, and drop casting on textile substrates as the active layer; however, these methods are constrained by the inhomogeneity and weak bonding of the coating.[80] It has been demonstrated that ALD makes it possible to produce conductive materials with anisotropic stretchability and conductivity on textiles, which were suggested for strain and pressure sensing.[80,81] For emerging manufacturing, atomic-level techniques offer excellent accuracy at near-atomic size, meeting the needs for functionality, flexibility, and down-scaling.[82] Hydroxyl groups are necessary as reactive sites to initiate ALD chemistry and covalently bond the coating to the surface of the polymer to create an ALD film of superior quality. Alternatively, the ALD technique can also deposit polymers without reactive sites. Infiltration is the first process for the growth of ALD films on these polymers because ALD precursors with small molecular diameters can pass through the pores and nucleate on the functional groups of the substrate.

In addition to being used in everyday life, fiber materials are also employed in the creation of cutting-edge materials and production techniques.[78,80] Smart textiles and fibers have attracted significant interest in wearable technology in recent years.[80,83] Due to certain problems with the elasticity, wearability, and durability of fabrics, a significant amount of research is being done on creating supercapacitors using elastic fabric treated with carbon because of its low cost, practicality, flexibility, low weight, and good electrochemical performance.[84] In contrast to rigidity, flexibility is the capacity to tolerate deformation from external forces, which includes stretching, twisting, bending, folding, or their combination.[85] Owing to their high flexibility, low cost, and rapid rate of charging and discharging, fabric-based supercapacitors are excellent choices for wearable applications. Furthermore, fabric-based supercapacitors have demonstrated superior mechanical, thermal, and electrochemical qualities, in addition to great flexibility and longevity.[84] Consequently, in today's technology, they show the ability to be flexible on smart devices, which is becoming increasingly crucial.

Many studies have been carried out recently to examine the formation and development of metal oxides, while using the ALD technique on a range of polymer substrates, confirming the high degree of flexibility of this technique.[86,87] However, despite its good film quality control, the sluggish rate of deposition, high cost and low throughput of ALD are obstacles preventing its scaled-up application. On the one hand, roll-to-roll ALD of thin films is the final goal in achieving mass production using the ALD method for coating flexible substrates such as those

utilised in organic PV and organic LEDs (OLEDs).[88,89] These opportunities also include the establishment of industrial roll-to-roll ALD in a variety of applications based on flexible polymer substrates using in flexible electronics, such as flexible sensors and energy storage. Only very flexible polymer substrates (such as fibers and textiles) can be processed using this roll-to-roll ALD growth system. It is evident that it can provide an advantage in terms of processing speed to achieve the optimal mass production line continuously.

ALD growth on polymeric materials

In the case of polymer materials, atomic layer deposition offers a major advantage over all other deposition methods. Once the coating layer is deposited at relatively moderate temperatures, it has good uniformity, high density, and flawless coverage on the substrate.[49,55] The ability to apply extremely thin layers on polymers *via* ALD has attracted wide interest given that it can be used to apply protective layers, coatings for optics, or even enable surface control to endow polymer surfaces with certain qualities.[50,90] Polymers at the microscopic level can be thought of as porous materials,[60,91] which are increasingly being used for numerous significant applications and optimised using atomic layer deposition,[91] including solar cells,[92,93] lithium-ion batteries,[94,95] advanced filtration materials, flexible electronic circuits, food packaging, sensors, composite reinforcement, membranes for biological capture and protection,[11,96,97] and organic light emitting diodes (OLEDs).[98–102] The polyethylene terephthalate and polyethylene naphthalene polymers are capable of being used as flexible electronics substrates.[103,104] Moreover, the electrospinning approach can be used to create a substrate of a 3D nanonetwork-structured polymer template, which allows the creation of materials made of ALD with a three-dimensional nanonetwork architecture, expanding the range of possible advantageous technological applications.[105] Typically, ALD is applied to coat polymers at a comparatively low temperature of below 150 °C[106,107] using materials such as Al_2O_3, ZrO_2, TiO_2, and HfO_2.[108–110] The correct application of the ALD procedure settings is required to generate a thin film coating of superior quality. Given the fact that surface reactivity and other substrate parameters are crucial in ALD, it is necessary to consider the way in which ALD reacts on the materials used as electrodes.[4,87] Thus, it is crucial to comprehend the ALD growth mechanism given that it enables the precise adjustment of the ALD process, resulting in deposited films with the best qualities.

It has been demonstrated that polymeric materials typically have a low melting point and are prone to degradation at high temperatures. This phenomenon is avoided in the typical ALD procedure, which enables the deposition of a wide range of ALD materials at relatively low temperatures. Furthermore, the thin layer formed by the ALD method on a polymer substrate can achieve excellent cohesiveness at the interfacial region with an extraordinarily smooth surface and a conformal coating. It can also improve the thermal and dimensional stability by creating a stable and strong skeleton within the polymeric matrix.[111] In comparison to other processes such as chemical vapor deposition, the ALD technique can be regarded as a highly compatible process for a wide range of polymeric substrates. All-polymer-based energy storage systems possess substantial inherent advantages compared to many of the batteries that are already in use in terms of affordability, adaptability, flexibility, and environmental friendliness.[112] The comparatively low cost of polymers is advantageous for diverse applications involving polymeric materials and the expansion of ALD materials.

The external surface shape and pore structure of pristine and Al_2O_3–porous polypropylene hollow fibre (PPHF) membranes were examined using SEM. The ALD approach for thin-film growth was used to change the dimensions of the pores in a nanoporous alumina membrane, while maintaining a narrow pore distribution.[113] There were no discernible particles on the outer surface of the pristine membrane, which showed a clean net-like structure (Fig. 5(a)). Following 50 cycles of Al_2O_3 deposition (Fig. 5(b)), no change in shape was noticeable in the external surface compared to the virgin membrane. However, a few tiny granules developed on the outside of the membrane with an increase in the number of ALD cycles (Fig. 5(c)). Al_2O_3 particles with a greater diameter were seen when the number of ALD cycles of Al_2O_3 was increased to 100 cycles. The Al_2O_3 nanoparticles gradually covered the outer surface of the membrane, and after 200 and 300 cycles of Al_2O_3 deposition, the surface became coarser (Fig. 5(d) and (e), respectively). After 400 cycles of Al_2O_3 deposition, the pores in the membrane were nearly entirely blocked because no pores could be seen at the same level of enlargement (Fig. 5(f)), suggesting that the ALD cycles can be modified to manage the average size of the pores in PPHF membranes. The presence of extra particles on the exterior of the Al_2O_3–PPHF membrane, as shown in Fig. 5, suggests that the formation mechanism of surface reactions came after the ALD process, thus limiting it. The pore shapes and outer surface morphologies were preserved, in addition to the pore diameters. During ALD, Al_2O_3 was found to grow conformably along the pore wall.[98,114] Moreover, an ultrathin Al_2O_3 ALD layer was shown to have a favourable effect on the wettability of a polymer-based separator, which ultimately led to a stronger ionic conductivity, in an effort to achieve the optimal

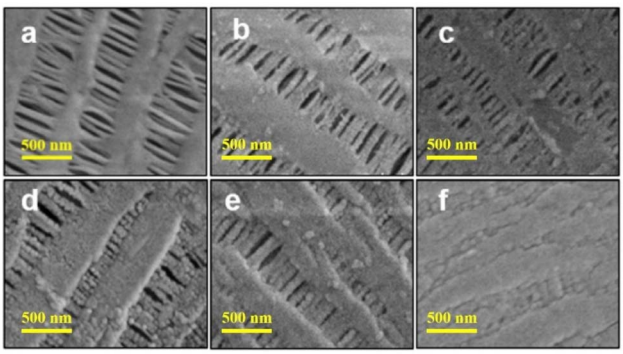

Fig. 5 SEM images showing immaculate (a) and porous polypropylene hollow fibre membrane with the deposition of Al_2O_3 at (b) 50, (c) 100, (d) 200, (e) 300, and (f) 400 cycles (reprinted with permission from ref. 48 copyright 2017, The Chemical Industry and Engineering Society of China, and Chemical Industry Press).

battery performance.[115] The most beneficial feature of the ALD technique in microporous engineering is that it allows fine control of the ALD cycles, which allows the accurate customisation of the pore size on the outer surface of membranes.

The inset in Fig. 6(a) displays a digital image of a 5 mm-diameter activated 3D-printed nanocarbon electrode. The related scanning electron microscopy (SEM) images of the 3D electrode at various magnifications are shown in Fig. 6(a). The electrode is made up of tightly packed fibers connected within a network. The length of the fibers range from a few to tens of micrometers and in diameter from tens to a few hundred nanometers. Dimethylformamide (DMF) exposes the carbon fibers by partially removing the polylactic acid (PLA) fillers used to bond the nanocarbon in 3D printing filaments. The overall electrochemical activity is increased by this activation phase, which also increases the heterogeneous electron-transfer rate. The appearance of the surface of the three-dimensional electrode with an aluminium oxide ALD layer obtained in 80 cycles is shown in Fig. 6(b). A distinct texture can be seen in the Al_2O_3-coated fibers when comparing the highly magnified pictures in Fig. 6(a) and (b). It is acknowledged that the slight variation from these SEM pictures is insufficient to support the presence of the Al_2O_3 coating because it its extremely thin on a nanometer scale in comparison to the fiber diameter on a scale of hundreds of nanometers.

Polymers that lack functional polar groups and have a dense crosslinking of the polymer chains are considered challenging and undesirable for use in ALD coating. This is because it is difficult for precursor nucleation *via* the infiltration mechanism to occur during the initial stage of growth. A macromolecule is a structure composed of several repeating units, whereas a polymer is a large molecule or macromolecule made up of many subunits.[60,117] Polymers are made up of several chains of polymers with spaces between them that are contained by microporous structures. If the polymer surface lacks functional –OH groups, the initial growth mechanism on its surface without hydroxyl groups can proceed by the infiltration of the precursor molecule into the polymer subsurface. As a result, it is possible to state that polymers can generally be coated using the ALD technique. However, the presence of a barrier layer on the polymer surface, such as a wax layer, whether deliberate or naturally present, can be regarded as an obstacle during the ALD coating process.

In terms of a polymeric surface that will be coated by materials *via* ALD, the required extra care for the surface preparation is cleaning the surface using an ultrasonic cleaner and ethanol (CH_3CH_2OH) as a liquid cleaner.[118] Polymers can be cleaned twice with new CH_3CH_2OH solutions, for 20 and 10 min each. The ultrasonic power and the temperature are set to 80 W and 30 °C, respectively. Subsequently, the polymers are dried in a reduced pressure oven for 1 h with the temperature of 50 °C. These processes ensure that fatty contaminants may be eliminated, allowing the polymeric surface to interface directly with the precursor and reactant during the ALD coating process.

The pictures of bare polyethylene terephthalate (PET) (Fig. 7(a)) and PET-coated TiO_2, Al_2O_3, and dual layer of Al_2O_3/TiO_2 *via* ALD are shown in Fig. 7(b)–(d), respectively. The uppermost exterior of bare PET reveals structures that resemble particles and have wavy patterns (Fig. 7(a)). The degree of coarseness diminished in the presence of the ALD layers, and it was dramatically reduced on the surface coated with more ALD film layers. It was demonstrated that PET coated with an Al_2O_3 layer is finer, which obviously implies that the Al_2O_3-covered surface has greater coverage than the TiO_2 film. The existence of an Al_2O_3/TiO_2 bilayer film can even improve the smoothness of the surface (Fig. 7(d)), demonstrating that it is possible to efficiently manufacture TiO_2 on the Al_2O_3 layer, which acts as an additional buffering layer.

Fig. 7(e) displays the contact angle, representing the surface wetting ability. ALD coating with ~50 ALD cycles transformed polymers with hydrophobic properties into hydrophilic.[120] The existence of hydrophilic sites linked to reactive oxygen increases the wetting behavior, as demonstrated by the corresponding decrease in the water contact angle. The angle of the Al_2O_3/TiO_2 bilayer-structured coating was smaller in comparison to that of the titanium dioxide film, which implies that the existence of a higher density of responsive functional –OH groups is beneficial for the water compatible interaction.[121,122] It could be stated that the early hydroxyl functional groups are present on the exterior for the subsequent reactivity of H_2O injection on the Al_2O_3 layer.[33,123]

The hydroxyl groups in the prior layer (*i.e.*, Al_2O_3) film may interact with the tetrakis(dimethylamino)titanium molecule, resulting in the normal growth of TiO_2. Substrate-inhibited ALD growth appears to be the type of TiO_2 layer deposition on Al_2O_3.[33,124] This is because tetrakis(dimethylamino)titanium (*i.e.*, four $N(CH_3)_2$) has more ligands than trimethylaluminum (*i.e.*, three CH_4).[33,125] These ligand exchange processes can increase the concentration of water-compatible functional –OH sites on the Al_2O_3/TiO_2 bilayer. This result suggests that the

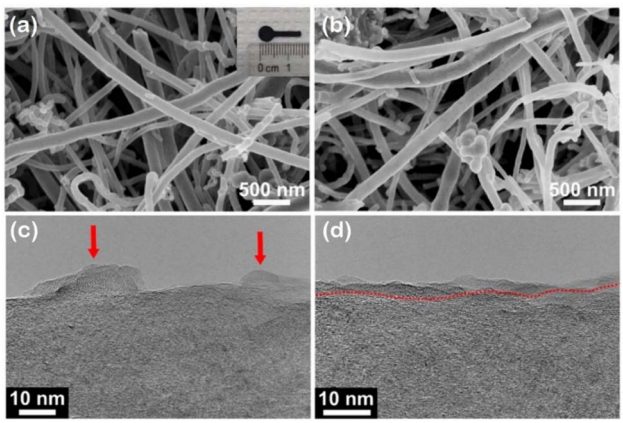

Fig. 6 SEM images of (a) pristine and (b) printed three-dimensional nanocarbon electrode covered with Al_2O_3 in 80 ALD cycles. A photo of the nanocarbon electrode printed in three dimensions following the process of dimethylformamide solvent activation is displayed in the inset in (a). (c) Blob-like islands visible in high resolution-transmission electron microscopy (HR-TEM) images taken at various points along the 80 cycles of printed three-dimensional nanocarbon electrode covered with Al_2O_3 (shown by arrows) and (d) continuous Al_2O_3 layer (denoted by the red line) that is isolated from the surface of carbon (reprinted with permission from ref. 116 copyright 2021, the American Chemical Society).

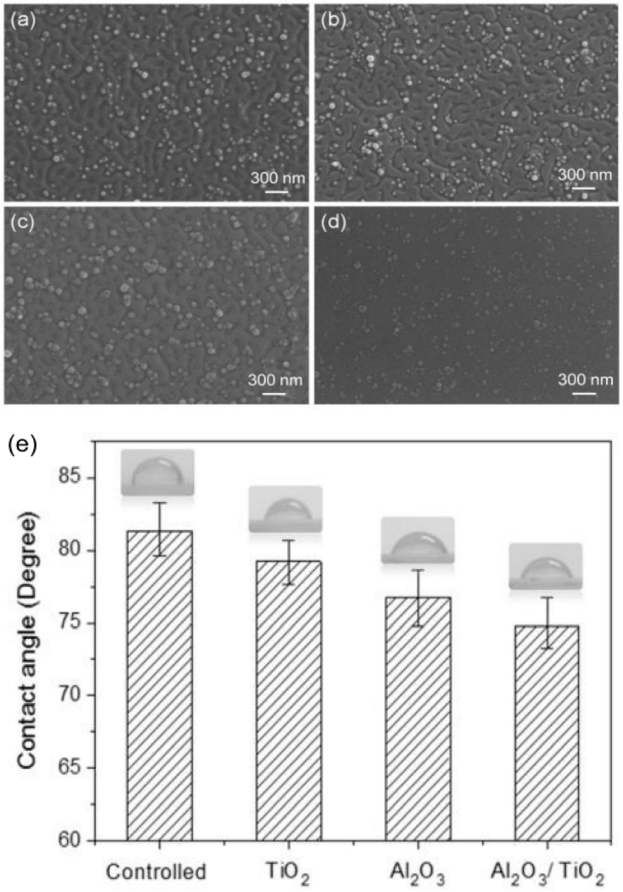

Fig. 7 SEM images of (a) PET without coating and PET surface with coatings of (b) TiO_2, (c) Al_2O_3 after 100 cycles of ALD, and (d) Al_2O_3/TiO_2 multilayer with 100 cycles of ALD for each layer. (e) Contact angles for the oxide-coated PET and uncoated PET (reprinted with permission from ref. 119 Copyright 2017, Elsevier B.V.).

Al_2O_3 layer could be a foundation layer to promote the following ALD formation of elements that are difficult to deposit. ALD of Al_2O_3 and TiO_2 has been demonstrated to improve the wettability of polymers, which can have a favourable impact on battery separator applications. Ceramic nanocoatings (*e.g.*, Al_2O_3 and TiO_2) significantly lowered the barrier to ionic transport across porous polymeric separators. Meanwhile, the enhanced ionic conductivity was primarily caused by the greater Li^+ ionic flow through the porous separators due to the improved electrolyte wettability of the ceramic coating. This is because a well-wettable separator enables lithium ions to easily travel between the electrodes, *i.e.*, the anode and cathode, which immediately affects the electrochemical characteristics of batteries.

The ALD growth mechanisms on polymer surface with reactive sites

The nature of the substrate controls the reactivity in ALD, where the formation of the first layer is often caused by different nucleation sites, while the production of the first growth layer may cause a change in chemistry.[126] Gas diffusion towards the substrate surface, surface absorption, reaction, desorption, and by-product diffusion are all components of the ALD mechanism.[127] ALD is an ideal candidate for decorating nanostructured surfaces because of its ability to conformally coat ultrathin films at very low temperatures on complex three-dimensional structures.[30,128] ALD requires an abundance of groups that are reactive (*i.e.*, –OH) to aid the early development of coatings, which are found naturally on various polymers such as cotton, polyvinyl alcohol (PVA), and rayon.[129] If the number of reactive sites is low, the first phase of growth starts by the ALD seed layer (*i.e.*, ALD growth on graphene oxide).[130] Reactive surface sites that are prone to ALD nucleation, such as –OH and C=O, must generate consistent, conformal film coverage with negligible subsurface growth.[11,119] However, ALD growth with precursor penetration and subsurface inorganic nucleation may have a negative impact on the material characteristics.[131,132] It can be concluded that the presence of numerous reactive sites with dense surface groups is required to achieve perfect growth *via* from the initial deposition to normal growth.

Fig. 8(a) depicts the starting scenario of Al_2O_3 formation on an SiO_2 surface (top left corner); the –OH groups that are naturally present on the substrate are exposed to a pulse of trimethylaluminum (TMA). The depositing process is a self-limiting reaction because through contact with the –OH groups on the surface, the TMA molecules are chemisorbed. After all the available –OH sites are occupied, no further TMA

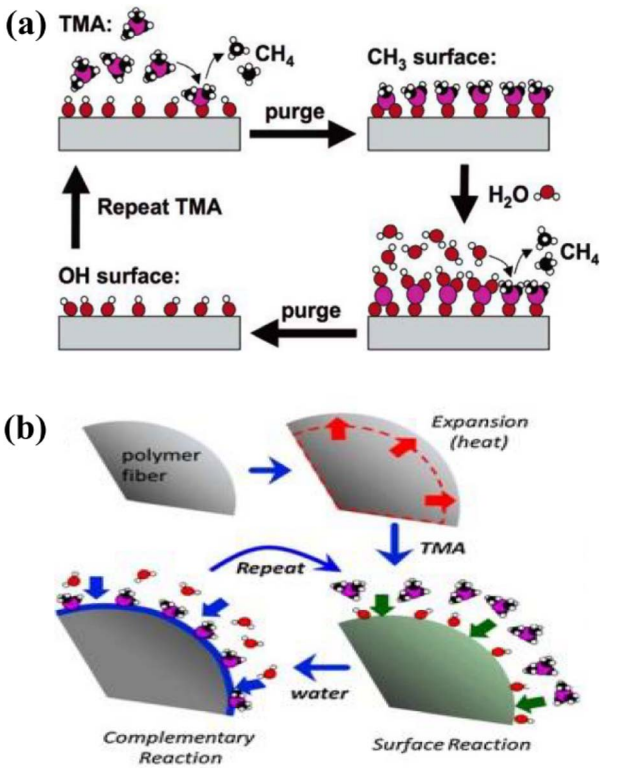

Fig. 8 (a) Diagram of an ALD cycle, self-limited ALD, showing layer-by-layer controllable construction of an Al_2O_3 layer from TMA and H_2O precursors (reprinted with permission from ref. 133 copyright 2007, the American Chemical Society). (b) Cotton fiber surface with abundant –OH groups exposed to ALD (reprinted with permission from ref. 12 copyright 2013, Elsevier B.V.).

can be absorbed (Fig. 8(a), top right). Following exposure trimethylaluminum, the reaction chamber is evacuated using a pumping system, and then a pulse of H_2O vapour is added (Fig. 8(a), bottom right). The remaining methyl groups are hydrolyzed when the adsorbed trimethylaluminum combines with H_2O gas. The resulting surface interaction causes the production of a (sub)monolayer of alumina. The initial Al_2O_3 film is terminated by OH groups in the lower left corner (Fig. 8(a)). Consequently, the ALD procedure might be restarted depending on the required thickness. These growth methods are analogous to the ALD initial growth of Al_2O_3 on the surface of the natural cellulosic cotton polymer, which contains an enormous density of reactive surface groups. However, both SiO_2 and cotton substrates have different features, in which the polymer surface is easily stretched due to heat, resulting in the formation of micropores. Fig. 8(b) depicts a schematic diagram of the ALD growth of Al_2O_3 on cotton fibre, which contains many –OH groups. A substrate containing abundant reactive sites promotes rapid ALD growth, in which trimethylaluminum exposure forms terminal aluminium methyl linkages on the substrate, which react and oxidise during future H_2O vapour injection (Fig. 8(b)).[12,134] Furthermore, for additional perspectives on the evolution of ALD on polymers, it is encouraged to read the review papers by Parsons *et al.*[12] and Guo *et al.*[135] In addition, the growth mechanisms in association with the evaluation of Fourier transform infrared spectroscopy (FTIR) characterization are shown in Fig. 9and their explanation.

The first cycle of deposition an Al_2O_3 atomic layer was demonstrated using trimethylaluminum and ozone, and the final (10th) step of Al_2O_3 using trimethylaluminum and H_2O (Fig. 9). Fig. 9(a) depicts the differences in the FTIR spectrum obtained after the final water injection during Al_2O_3 deposition using trimethylaluminum and H_2O. A positive characteristic was discovered, in accordance with the O–H stretching vibration from the additional AlOH* hydrophilic sites (at 3640–3730 cm^{-1}). However, negative absorbances were detected at 2920–2980 cm^{-1} due to the C–H stretching vibrations and at 1212 cm^{-1} related to Al–CH_3 (Fig. 9(a)). Both these negative absorbance properties resulted from the elimination of $AlCH_3^*$ species. Fig. 9(b) depicts the infrared spectrum for the following trimethylaluminum injection, indicating that trimethylaluminum eliminated the AlOH* species and introduced $AlCH_3^*$. Fig. 9(c) demonstrates a significantly altered spectrum, with new positive absorbance characteristics observed at around 1200 to 1700 cm^{-1}. Long-term ozone exposure did not eradicate all the C–H characteristics. Several tiny absorption patterns at 2923 and 3016 cm^{-1} for the C–H stretching vibration partly resulted from the minor frequency changes. Furthermore, the intensity of the O–H stretching vibration at 3734–3778 cm^{-1} decreased in comparison to the intensity shown in Fig. 9(a) following H_2O exposure. Fig. 9(d) indicates that the novel absorbance characteristics produced by the ozone injection were totally eliminated by the subsequent trimethylaluminum injection. Trimethylaluminum injection transformed the absorbance from the C–H stretching vibration (2820–2970 cm^{-1}) and the distortion of methyl (1212 cm^{-1}). The TMA injection also resulted in the disappearance of the absorbance between 3734 and 3778 cm^{-1} from the O–H stretching vibration.

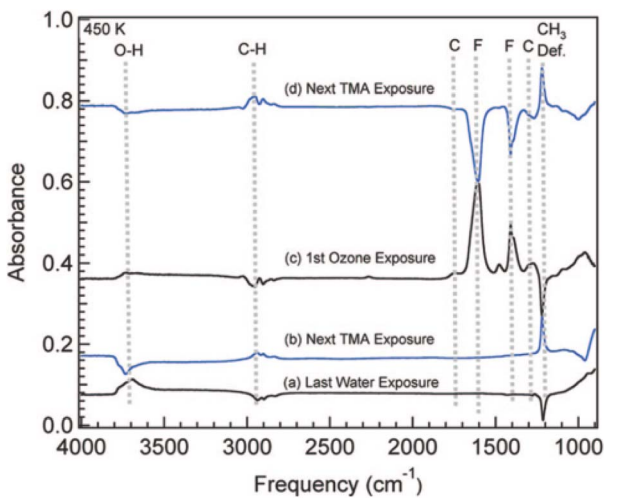

Fig. 9 Difference in FTIR spectra following (a) the most recent water exposure, (b) subsequent exposure to TMA, (c) first exposure to ozone, and (d) subsequent exposure to TMA. All exposures were carried out at 450 K. C = carbonate and F = formate (reprinted with permission from ref. 136 copyright 2008, the American Chemical Society).

The ALD growth mechanisms on a polymer surface devoid of reactive sites

The initiation of film growth is a key feature in atomic layer deposition. Precursors are normally required to react with the active sites in the substrate; thus, the absence of these reactive sites on the surface may lead to a significant delay in nucleation for the formation of a layer. Usually, surface imperfections are where nucleation begins for an inactive material. In this situation, early atomic layer deposition typically leads to uneven growth and the creation of deposition spots that are not continuous.[137,138] The resulting deposition spots keep growing with an increase in the number of atomic layer deposition cycles, ultimately coalescing to create an uninterrupted layer. ALD of Al_2O_3 with trimethylaluminum/H_2O precursors has been experimentally proven to be deposited on many different substrates, including polymers without polar groups (*e.g.*, polypropylene and polyethylene),[139] which are activated by the diffusion mechanism in the initial few cycles.[132,140,141] Although they are capable of being coated, the existence of polar groups is required to generate high-quality thin films. For understanding gradients of atomic layer deposition in microporous polymeric materials, polymers that are reactive provide an excellent model system given that the first step in the formation and development of metal oxides may proceed smoothly on their surface.[142] In many hydrophobic polymers, such as polypropylene and polyvinylidene fluoride, their inert surface inhibits the spontaneous growth of an atomic layer during the initial phase. This characteristic growth mechanism also normally happens on membranes made of polymers (*e.g.*, polyamide, polysulfone, and polyvinylidene fluoride membranes) with a pore size of

a few nanometers (*i.e.*, micropores of less than 2 nm), which can be used for nanofiltration, vapour permeation, and separation of gases.[143,144] Thus, a significant number of deposition cycles or pre-treatment prior to the ALD process such as non-thermal plasma treatment and sensitisation of the surface is required to facilitate the initial deposition through the formation of nuclei and further growth.[118,142,145] The essential function of plasma-induced surface modification in simplifying the process of atomic layer deposition on a polypropylene-based membrane is that the plasma-activated polypropylene membrane used as a separator in LiBs required just 20 deposition cycles to achieve a continuous TiO_2 deposition layer.[144] Surface pre-treatment with non-thermal plasma was employed to produce reactive substances on the inert membrane surface, which was functionalized as a battery separator, considerably facilitating the creation of conformal and uniform coatings in the minimum number of cycles.[146,147] Improved wettability might efficiently promote the electrolyte ion flow *via* the separator channels without sacrificing pore size, hence improving the electrochemical performance of LiBs.[146]

The Al_2O_3 series of reactions uses trimethylaluminum and H_2O on various reactive site-free polymers such as polyimide and polypropylene. It was noted that the interaction of the precursors and reactants with the substrate is largely dependent on the initial polymers, precursors, and precise process conditions. Trimethylaluminum infiltrates the topmost area of the surface of inert polymers, such as PP, after which it interacts with H_2O during the next half-cycle stage to produce nuclei on the polymer surface or underneath it. Meanwhile, in polymers with an abundance of reactive groups, the top surface of the polymer may be the only area where the ALD reaction occurs. To create an aluminum–oxygen–alkyl unit and break the hydrogen bonds between adjacent chains, the carbonyl site is anticipated to work in tandem with trimethylaluminum, encouraging additional trimethylaluminum diffusion into the subsurface area.[148] During the infiltration phase, the molecular weight close to the outermost layer of the polymer substrates decreases due to the breaking of the polymer chains.[117] By increasing the amount of reactive groups on the surface of polymers, the reduction in the average chain length of the polymer initiated growth. This is because the first coordination of the carbonyl site with the precursor is beneficial for new polar groups to emerge as a result of the breaking of the polymer chains.

The polymer substrate is depicted in Fig. 10 as circles that are closely spaced with a greater free volume in the area close to the surface. The near-surface of the polymer film is where trimethylaluminum molecules are trapped, which allows the deposition to proceed although the polymer does not possess any initial hydroxyl groups. As seen in Fig. 10(b), additional exposure to water causes a reaction with trimethylaluminum, which leads to the creation of nucleation clusters of Al_2O_3. These Al_2O_3 seed clusters fill the gaps among the chains of polymer as they expand in the area close to the surface as a result of increasing trimethylaluminum and water exposure. Fig. 10(c) illustrates how the Al_2O_3 ALD layer transforms into an almost uninterrupted layer. As seen in Fig. 10(d), successive exposure causes the underlying ALD Al_2O_3 polymer film to

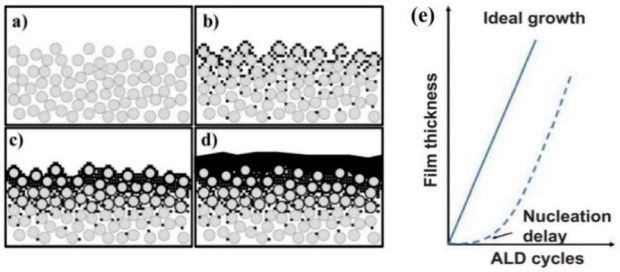

Fig. 10 Concept of ALD of Al_2O_3 on polymer sheets, demonstrating (a) loosely packed circles, showing the cross-section of a polymeric film, (b) clusters of Al_2O_3 nucleation are created in the vicinity of the surface *via* the interaction of H_2O with trimethylaluminum, (c) Al_2O_3 clusters coalescing and the gap between chains of polymers closing, and (d) normal growth of Al_2O_3 on the polymer (reprinted with permission from ref. 149 copyright 2005, the American Chemical Society). (e) Diagram of the common non-ideal causes for nucleation-delay in ALD (reprinted with permission from ref. 137 under a Creative Commons Attribution 4.0 (CC BY) license).

gradually grow. This uninterrupted coating ought to successfully prevent the additional penetration of TMA and H_2O reactants into the area close to the surface. After ten to fifteen ALD cycles, the changes in mass determined using a quartz crystal microbalance (QCM) show that the infiltration of TMA among the polymer chains is hindered.[149] Because highly dense reactive sites will be available for each phase of the half-cycle ALD process, reaching this stage will eliminate any obstacles for the subsequent stages of ALD growth.

As seen in Fig. 10(e), nucleation delay appears to have occurred on the polymer surface with a low functional group density or on the polymer without functional groups. This is due to the fact that the diffusion mechanism involving infiltration will be utilised in the initial cycles for polymers lacking functional groups. However, the surface of polymers with smaller amounts of functional groups will experience initial expansion through island growth. The first ALD growth on graphene oxide, which has a low density of functional –OH groups, is comparable to this growth mechanism.[130,158] In the case of the ALD of Al_2O_3 using trimethylaluminum and water, graphene oxide is a great seeding layer that promotes regular nucleation and the creation of smooth, closed thin films.[130] The nucleation delay brought on by the defective condition of the substrate surface can be thought of as growth that is started by a few ALD cycles to establish a baseline in the interfacial layer. Reactive surface groups, such as –OH groups, should be densely distributed across the substrate surface to form the necessary surface for the first ALD growth to immediately develop a normal ALD layer.

Roles of ALD and polymer materials in lithium-ion batteries

A cutting-edge thin film technological development is atomic layer deposition, which offers complex control of the deposited layers.[159] In the case of lithium-ion battery electrodes, nanoscale materials have demonstrated greater durability than similar bulk materials as electrodes.[160,161] According to research, ALD-

coated graphite anode electrodes were found to have significantly increased durability compared to both electrodes made of uncoated graphite and small particles of active graphite powder, which were separately coated by atomic layer deposition.[4] This was attributed to the ALD protecting the active powder surface in the electrodes and the undamaged interparticle electron conduction channels.[4] As protection layers with stable electrochemical properties, atomic layer deposition oxide coatings that are very thin on surfaces of electrodes may inhibit the dissolution of their metal components and decrease the electrolyte reactions on their surface, leading to a significant improvement in the cathode performance in LiBs.[146] Additionally, by altering the exterior of the separator of polymeric LiBs and creating an artificial solid electrolyte interface (SEI), atomic layer deposition is capable of functionalizing materials to elevate the efficiency of LiBs. This will help maximise the movement of lithium ions from the cathode to the anode, and conversely throughout the operations of charging and discharging. Table 1 summarizes the use of polymers and ALD materials for lithium-ion battery applications. These polymer materials include wood fibers, polyurethane, polyethylene, polypropylene, polyvinylidene fluoride-hexafluoropropylene (PVDF-HFP), and a trilayer PP/PE/PP separator (Celgard). The ALD materials used for coating these polymers are Al_2O_3, ZnO, and TiO_2. The precursor of TiO_2 layer is created from titanium isopropoxide (TIP) and water.

The shift in volume that occurs during battery operation is the cause of the natural SEI reformation phenomenon. Cycles of charge and discharge may cause the anode to be crushed, which will cause the battery to fail given that the disintegration of the anode will decrease the movement of electrons and ions. Additionally, the interaction between the electrolyte and the surface area of new or fresh cracks in the active material of the anode causes an issue with the production of a solid electrolyte interfacial (SEI) layer.[162] The existence of an artificial SEI created by atomic layer deposition can prevent repeated SEI generation in flexible batteries. This is because the ALD materials an artificial SEI that are deposited onto the anode, which is stacked on a polymer platform, do not alter the bending mechanism of the substrate. Furthermore, ALD can be utilised to stabilise the electrodes, and perhaps even the electrolyte components by depositing protective layers.[163] It is evident that the thin films produced by ALD can positively impact efforts to improve the performance of batteries.

The procedures for the formation of an SEI depend on the thermodynamic parameters involved in its formation. Impurities (including trace water), additives, solvents, and lithium salts will all be less prevalent in the electrolyte when its lowest empty molecular orbital is lower than the Fermi energy of the anode.[164] The anode surface is eventually covered in soluble and insoluble compounds as a result of these competing reduction processes.[164] Therefore, the chemical surroundings have a significant impact on the complex composition of the SEI, which grows and degrades in response to structure-related alterations in the electrode during the battery operation.[164] It is known that one of the primary reasons why electrodes deteriorate is the formation of a solid-electrolyte interphase (SEI) during lithiation reaction cycles.[4] The electrode capacitance is further weakened by side reactions during the cyclic charge/discharge operations.[4] Thus, an efficient method to lessen these effects is to apply a thin coating on the electrodes. This can be achieved using the advantage of the ALD method, which produces a thin coating at the angstrom-level that is extremely conformal and uniform.

In Fig. 11, the stability of silicon nanowires (b) and thin film and particles (a) after repeated lithiation and de-lithiation is schematically compared. It was demonstrated that silicon nanowires outperformed silicon thin films and particles in lithium-ion batteries. Because of their easy strain relaxation and effective electron transport along each nanowire, silicon nanowires could prevent pulverisation and contact loss. In the effort to improve the structure and properties of nanowires for LiBs, the atomic layer deposition process can be an ideal option because it can be used to deposit coating materials with an angstrom-level thickness on complex structures with features of great uniformity and conformality on the substrate.

The core of contemporary electronics is nanofabrication technology, which depends on thin film deposition processes.[56] The exponential proliferation of gadgets, electronic devices, and their use in daily life has made energy storage devices more significant.[84] The creation of flexible, wearable, high-mass consumption printed electronic components that are woven into textiles to create smart clothing is an emerging trend.[77] The research community is urged by the negative impacts and

Table 1 ALD materials with involvement of polymers for LiBs

ALD material	Substrate	Precursor	Temperature (°C)	Discharge capacity (mA h g^{-1})	Role	Thickness	Reference
Al_2O_3	Wood fiber	$Al(CH_3)_3/H_2O$	150	442	Anode	5 nm	150
Al_2O_3	PVDF-HFP	$Al(CH_3)_3/H_2O$	70	98.88	Separator	30 nm	151
Al_2O_3	Celgard	$Al(CH_3)_3/H_2O$	80	1150	Separator	20 cycle	152
Al_2O_3	PVDF-HFP	$Al(CH_3)_3/H_2O$	80	170	Separator	10 nm	153
TiO_2	PP	TIP/H_2O	120	160.7	Separator	20 cycles	154
TiO_2	PE	TIP/H_2O	110	308	Separator	100 cycles	111
ZnO	Polyurethane	$Diethylzinc/H_2O$	150	5000	Anode	500 cycles	155
Al_2O_3	Celgard	$Al(CH_3)_3/H_2O$	80	150	Separator	25 cycles	156
Al_2O_3	PP	$Al(CH_3)_3/NO_2$	50	120	Separator	50 cycles	157

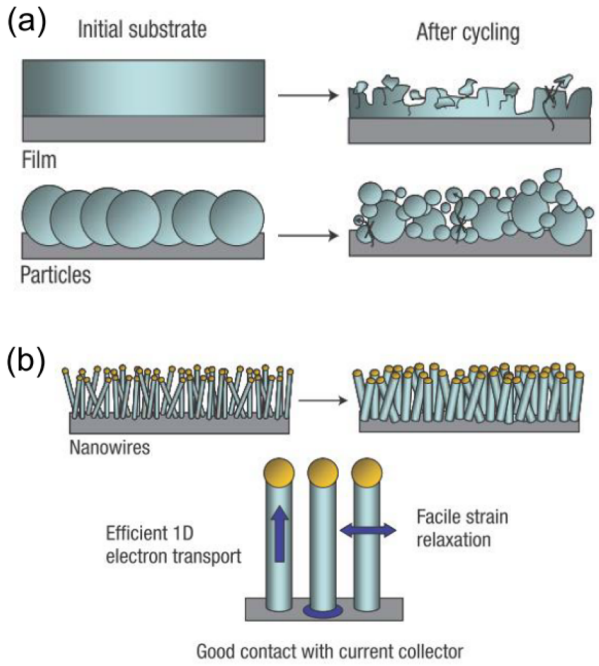

Fig. 11 Diagram showing the morphological alterations in Si, occurring during electrochemical cycling. (a) Cycling causes a 400% change in the volume of silicon anodes. Consequently, Si particles and films have a tendency to grind when cycling. The arrow shows that poor electron transport results from a large portion of the material losing contact with the current collector. (b) After cycling, nanowires (NWs) formed directly on the current collector do not crush or fragment into smaller pieces. Instead, the easy strain relaxation of the NWs enables them to grow longer and wider without shattering. Effective 1D electron transport is made possible by this NW anode arrangement, which connects each NW to the current collector (reprinted with permission from ref. 165 under a Creative Commons Attribution 4.0 (CC BY) license).

depletion of fossil fuels to look for sources of renewable energy and develop energy storage technologies to efficiently store the harvested energy.[84] ALD is known to have several positive impacts, such as (i) interfacial stabilization characteristics with a decrease in solid electrolyte interface generation, (ii) enhancing the mechanical integrity of the electrode, and (iii) reducing significant volume changes in the substances used for electrodes.[46] It is expected that ALD, a scalable and economical technology for altering the surfaces of materials, can successfully compete with traditional surface modification methods on a commercial level.[113] However, the advantages brought by the availability of ALD materials are insufficient for contemporary technologies. This is due to the fact that in real-world applications, characteristics such as light weight and flexibility become essential. Thus, it is imperative that organic polymeric materials be used in the endeavour to advance the ALD process for use in the future. Given the need for polymeric materials in a variety of uses, they are becoming crucial materials in contemporary technology. Polymeric substrates can generally be employed in ALD for lithium-ion batteries in three ways, as follows: (a) as sacrificial substrates that are not involved in the battery system; (b) as substrates that simultaneously function as anode components of the battery following a specific treatment (calcination); and (c) as substrates that subsequently directly occupy a position in the battery component (*i.e.*, separator).

When comparing the energy densities of several commercial rechargeable batteries, Fig. 12 makes it abundantly evident that Li-ion batteries are superior to other types of batteries. Despite having theoretically higher energy densities than Li-ion batteries, lithium metal batteries are known to have drawbacks such as low rechargeability and a high risk of fire or explosion from misuse.[165] Thus, it will be advantageous to reduce the battery size and develop a lighter battery due to the better energy density. These features are crucial for powering portable electronics, including flexible and wearable electronics. The endeavour to improve the electrochemical performance and safety of flexible energy conversion devices currently faces numerous obstacles, as follows:[167] (1) forming stable mechanical structures using very elastic electrodes; (2) flexibility in using solid/gel-type electrolyte systems and nanoscale active materials with powerful properties to guarantee safety; and (3) stabilized packaging materials with outstanding barrier qualities. Presently, the use of ALD materials is particularly significant in the field of electrical devices that are bendable, where extremely thin and superior films are required. The specifications for barrier layer coatings are extremely strict regarding moisture barrier application given that the coating must[19,101] (1) be conformal and continuous, (2) be free of pinholes, (3) be flexible, and (4) have a water vapor transmission rate (WVTR) as low as 10^{-6} g per m^2 per day (*i.e.*, for LEDs and solar cells). LEDs are the only devices that can meet these requirements. Additionally, it is widely accepted that it is possible to deposit a wide range of thin film materials that can

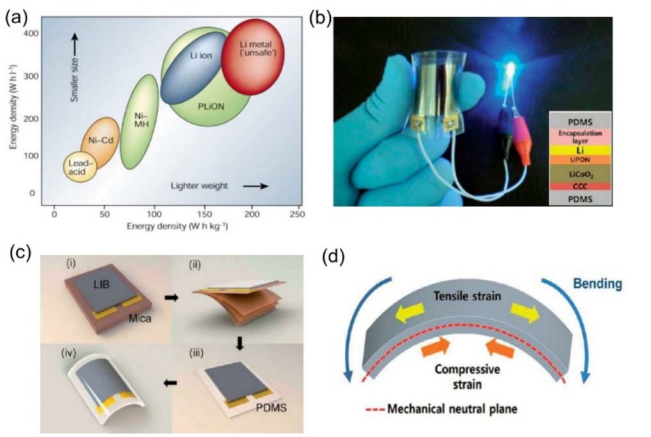

Fig. 12 (a) Comparison of the energy densities of several battery types using gravimetric and volumetric methods (reprinted with permission from ref. 165 under a Creative Commons Attribution 4.0 (CC BY) license). (b) Example of a flexible battery used to power an LED bulb. (c) Outline of the procedure for creating a completely bendable LiB using materials that are entirely in solid-state (LiPON as the electrolyte, $LiCoO_2$ as the cathode, and Li film as the anode, respectively) wrapped in a polymer sheet (PDMS) and (d) schematic showing the emerging strain caused by the bending of a flexible battery (reprinted with permission from ref. 166 copyright 2012, the American Chemical Society).

be helpful in the process of creating flexible battery components using ALD, which in turn can improve the battery performance.

A conductive layer must be included in non-conductive substrates for them to function as current collectors. In this case, metal deposition is the primary method used to create current collectors. Under polymer sheet wrapping, an LiB made entirely of solid-state materials that is completely flexible was created. A universal transfer technique based on sacrificial mica substrates was employed for the construction of a battery. Specifically, an Ni-based alloy was employed as the current collector after deposition on a mica substrate. The substance utilized for the current collector (*i.e.*, cathode) had an $LiCoO_2$ layer placed on top of it, and LiPON was added to serve as an electrolyte film. Subsequently, Li metal served as the anode/current collector. The encapsulation technique was the final stage of production on the mica substrate. Because of the upper protective encapsulating layer, the Li anode and LiPON solid electrolyte materials were shielded from oxygen and moisture, which would have accelerated the deterioration of the battery performance.[168] It was demonstrated that an excellent moisture permeation barrier was produced *via* the ALD of Al_2O_3 on a polymer with a thickness of 20 nm, specifically poly(2,6-ethylenenaphthalate).[98,169] The application of polymeric substrates in flexible electronics requires the use of a thin film deposition process at low temperature, creating superior moisture permeability barriers.[169] The thin film encapsulation layer must be both flexible and an effective moisture barrier to create a flexible device. Given that films obtained by ALD have been demonstrated to offer good protection against moisture degradation, aluminum oxide has been the preferred material for thin film encapsulation.[170,171] Water vapour transmission rate assessments can be performed as part of the barrier evaluation to evaluate the quality of films and their appropriateness for use in the encapsulation of flexible electronics.[101] Using adhesive tapes, the mica substrate of a thin film LiB was physically delaminated and peeled off. The bendable LiB was applied on a substrate made of PDMS polymer following substrate delamination. Lastly, to improve the mechanical stability, another PDMS sheet was wrapped around the flexible thin film LiB. In relation to the radius of bending, the LiB characteristics demonstrated sustainability for a flexible energy source with great performance. With an upper limit on the charging voltage of 4.2 V, the flexible LiB could deliver 106 μA h cm^{-2}.[168]

ALD on polymers for lithium-ion batteries

Polymer materials are made up of numerous repeating subunits and very massive molecules known as macromolecules. They can be either synthetic (such as polyethylene, polypropylene, polystyrene, and nylon) or natural (such as wool, hemp, silk, and natural rubber) and mostly made of carbon element chains. These substances fall under the category of soft materials that can be used as substrates for thin film deposition utilizing the ALD technique. The reason for this is that certain ALD materials (such Al_2O_3 and TiO_2) allow deposition at temperatures below 100 °C. Using calcination or dissolving techniques, the sacrificial polymer substrate can be eliminated to use the deposited layer to enhance the performance of Li-ion batteries. Organic materials can be carbonized *via* calcination at a high temperature (400 °C to 800 °C) in an atmosphere with noble gases such as Ar, He, and Ni. However, sacrificial polymer substrates can be completely eliminated by calcining in an oxygen-rich atmosphere at a high temperature. Thus, the process of ALD has been used in many different ways to deposit materials on organic materials, including polymers for energy applications. For example, polymers coated with ALD were calcined at high temperatures in the presence of noble gases (such as Ni, Ar, and He) before being used for LiBs. In terms of polymers that are functionalized as sacrificial substrates through the calcination process, which are then applied in the ALD growth processes on the substrate, natural polymers may be able to produce a better film than synthetic polymer substrates.[135,155] Natural polymers, such as cotton, contain a high density of functional OH groups, allow ALD materials to grow directly on the substrate. This growth process allows ALD films with superior quality to be achieved than ALD materials grown using diffusion growth mechanisms, which frequently occur on synthetic polymer substrates (*e.g.*, polypropylene). In ALD materials for LiB application, a good quality film formed by the typical natural polymer may result in an improved LiB performance. ALD has emerged as a promising approach for the production of cutting-edge LiBs in recent years, achieving uniform thin film coverings on powdered LiB materials and assemblies with adjustable thickness at the Å-level.[146,172] Given its special characteristics, it may be concluded that ALD is a vital procedure in endeavours to improve the performance of batteries.

Given that the separation process is managed by the size-sieving method, membrane-based separation is becoming increasingly significant in a variety of fields pertaining to energy, water, natural resources, and the environment.[18] Surface alteration of the electrodes and separators has been investigated as a viable method for enhancing the performance of LiBs.[146] A separator is a porous membrane placed between electrodes of opposing polarity, which allows ionic movement but inhibits electrode electric contact.[173] Although it does not participate in electrochemical reactions, one component that is crucial in LiBs is the separator, which has a direct effect on the safety and electrochemical characteristics of batteries.[174] Separators have been manufactured using a variety of materials, including cellophane, cellulosic papers, foams, nonwoven textiles, ionic exchange membranes, and microporous thin membranes made of polymeric materials.[173] By keeping the positive and negative electrodes separate, they avoid electrical short circuits and allow ionic charge carriers to move quickly, which is essential for completing the circuit during the passage of current in an electrochemical cell.[173,175] They should have the capacity to transport ions through intrinsic ionic conductors or electrolyte soaking, making them excellent electronic insulators.[173] Because of their advantageous electrochemical and mechanical characteristics, separators of porous polyolefins including polyethylene (PE), polypropylene (PP), and PP/PE/PP trilayers are frequently utilised for LiBs.[111] However, polymeric

separators have a few significant drawbacks, as follows: (i) melting or thermal shrinkage at high temperatures; (ii) low wettability towards nonaqueous electrolytes that contain Li salts; and (iii) poor compatibility with certain traditional electrolytes (such as ethylene and propylene carbonate (PC)).[111,146,154] This implies that one of the main issues with polymer-based battery systems is their poor cycling stability.[112] Batteries operate at a relatively high temperature but polymers are organic materials that are typically sensitive to high temperatures. This can result in mechanical instability and low conductive properties because of the charge–discharge mechanism, which causes thermal expansion, ultimately leading to molecular disintegration. Thus, one potential approach is to construct devices that can preserve the structural integrity of the battery components by improving the technique for managing the morphology of the ALD elements inserted into the polymers. Recent research has revealed that ALD of TiO_2 and Al_2O_3 enhances the wettability and thermal stability of separators based on polymers without any major limitations on mass transport.[146] It is evident that ALD can enhance the ionic flow between the anode and cathode electrodes and the safety of LiB operation using a polymer-based separator.

Porous films made of polypropylene (PP) have found extensive application as separator membranes in batteries and membranes for distillation, microfiltration, and ultrafiltration.[49] Given that ALD can be performed at a temperature below the melting point of polypropylene and is independent of the surface morphology of polypropylene, it is widely used in polypropylene film engineering. Furthermore, its use is primarily based on the state-of-the-art homogeneity and controllability of the coating layer at the atomic to nanometer scale.[49] Given that the entire surface of PP is made up of $–CH_2–$ and $–CH_3$ groups, its surface is comparatively inert to initiate ALD development. Instead, its pores allow precursors to permeate it, and subsequently trapped within the unfilled volume among its polymer chains, which is how the growth and nucleation of an ALD film on the normally porous polypropylene are primarily initiated.[49,176,177] Given their ability to absorb ALD materials through ligand exchange reactions as initial growth and infiltration growth mechanisms, polymer-based materials can be considered ideal substrates for the ALD process. This could be the reason why combining the ALD method with polymer-based substrates has significant potential for future exploration in a wide range of applications.

Films made of porous polyolefins (*i.e.*, polypropylene and polyethylene) that are less than 25 μm thick are commonly used as separator materials in commercial LiBs.[157] Despite the general dependability of separators for portable applications, two significant obstacles must be removed for energy storage in vehicles.[157] Initially, at high temperatures, the polymer separators melt and shrink.[157,173] One type of ceramic material that can shield polymer-based coated materials is ALD materials, such as Al_2O_3. If these materials are used to insulate polymer-based separators, they can lessen the shrinkage and melting of the separator, thus improving the battery performance. For instance, a battery temperature may increase due to an internal short circuit, causing shrinkage or melting, which can accelerate the internal propagation of the short circuit and produce Joule heating, which is very high, resulting in unwanted exothermic adverse effects on electrodes. Frequently, they cause disastrous events involving thermal runaway.[157,178] Secondly, because polyolefins are hydrophobic and have low surface energies, polymer separators are incompatible with certain typical electrolytes that contain solvents with high dielectric constants (such as propylene and ethylene carbonate), which results in wetting issues.[157,173] Al_2O_3 and TiO_2, which are deposited using the ALD process, have been shown to make the surface of the coated separator more hydrophilic. This improves the interaction between the electrolyte and the battery separator surface, allowing lithium ions to flow smoothly from the cathode to anode and *vice versa*. Consequently, it can improve the electrochemical performance of the battery.

As shown by the schematic in Fig. 13(a), on the entire surface of the microframework of porous polymers, an Al_2O_3 layer smaller than 10 nm is deposited (porous polypropylene (PP) separator (Celgard 2500)) without appreciably thickening the separator. Only the ALD technique can deposit such a thin film over a microporous membrane with a conformal 3D structure all over a 3D microporous framework. Crucially, even with a strong polar electrolyte and pure propylene carbonate (PC) as the solvent, the thin Al_2O_3 ALD coating allows good wettability, in addition to greatly reduced thermal shrinkage. The safety of lithium-ion batteries depends on the use of a separator; however, commercial separator batteries, such as polypropylene separators, have issues with limited electrolyte wettability, poor mechanical strength, and poor thermal stability.[179] Ceramic oxides such as TiO_2, Al_2O_3, and SiO_2 have been employed to coat PP separators to enhance their mechanical characteristics and resistance to heat.[179] It is important to note that numerous materials can be deposited using ALD, which can overcome the mechanical and chemical features of the separator and improve the battery performance.

In an attempt to improve the performance of batteries by modifying porous PE membranes used as separators through the use of ALD, TiO_2 thin layers made with H_2O and titanium isopropoxide (TIP) can be effectively produced on polymeric PE separator membranes.[111] Because of the ionic movement phenomena, the TiO_2 ceramic nanocoating greatly reduced the ionic diffusion barrier *via* the porous polymeric separator.[111] However, the ability of the ceramic coating to improve the electrolyte wettability led to an increase in the flux of Li^+ ions *via* the porous polyethylene-based separator, which was primarily responsible for the higher ionic conductivity.[111] Lithium ions can move between the cathode and anode more readily when a separator has strong wettability, which has a direct impact on the electrochemical performance of batteries.[173] Furthermore, when cycling at high temperatures, the separator of PE coated with TiO_2 improved the LiB performance.[111]

Titania was applied to PE membranes using a roll-to-roll ALD process mechanism with a linear roller velocity of 5 mm s^{-1} during the deposition process, with one hundred ALD cycles. This separator coated *via* ALD was employed to fabricate a device. To examine the deterioration of the pouch cell constructed with the separator coated with a ceramic, as shown in

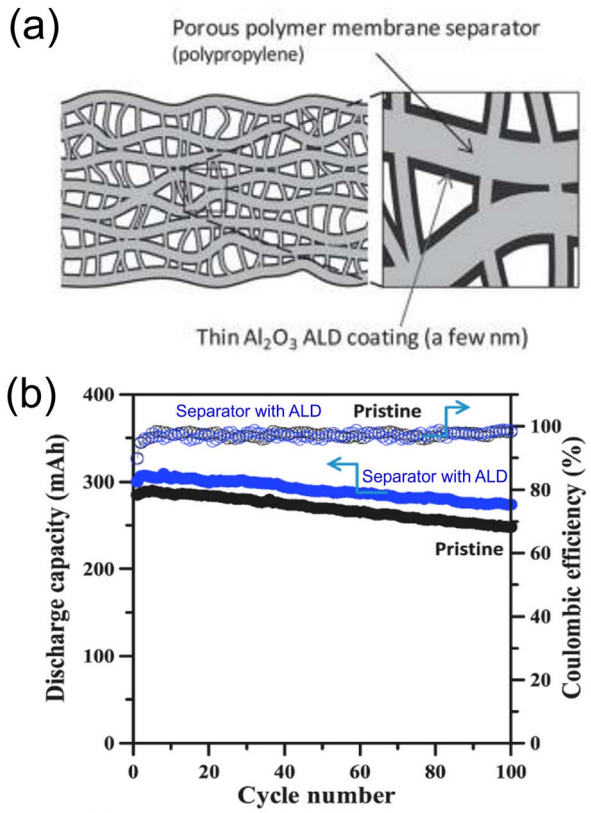

Fig. 13 Diagram of the cross-section of (a) a separator made from polymeric porous materials covered with ALD, in which the porous microstructure is coated with Al_2O_3 layer (a few nm) (reprinted with permission from ref. 157 Copyright 2012, WILEY-VCH Verlag GmbH & Co. KGaA, Weinheim). Charging and discharging curves of a typical pouch cell made with $LiNi_{0.5}Co_{0.2}Mn_{0.3}O_2$ (NCM)/graphite using pristine and separator coated with ALD. (b) Correlation of the battery cycle number with coulombic efficiency (at 55 °C) and discharge capacity (at 1 °C) (reprinted with permission from ref. 111 Copyright 2020, Elsevier B.V.).

Fig. 13(b), high-temperature extended cycling (*i.e.*, 55 °C) was also carried out at 1C. Fig. 13(b) shows that the pouch cell employing the bare polymer membrane had a lower accessible capacity during cycling. During high-temperature cycling, the $LiNi_{0.5}Co_{0.2}Mn_{0.3}O_2$ (NCM) cathode was typically both mechanically unstable and possessed low conductive properties. As revealed in Fig. 13(b), the capacity degradation became more obvious at elevated temperatures. The discharge capacity of the LiB using a separator without surface modification dropped to 12.9% of its original capacity after 100 cycles at 55 °C, while the LiB assembled with the separator coated *via* ALD showed excellent stability when cycling at elevated temperatures, with a reduction in its initial capacity by only 8.7% over the course of the extended cycling, as shown in Fig. 13(b). This result shows that the use of polymer membranes with a ceramic nanocoating (such as the separator coated *via* ALD) can significantly reduce the performance deterioration in batteries.

The overall film thickness remained unchanged following ALD coating, as shown by the cross-section pictures of the separator without coating (Fig. 14(a)) and separators with an Al_2O_3 atomic layer deposition coating after 50 and 100 cycles (Fig. 14(b) and (c)), respectively.[157] According to the FESEM picture in Fig. 14(a), the naked PP separator exhibited pores that resemble slits and were about 500 nm long and 50 nm wide. The aluminum oxide formation rate on polypropylene is anticipated to be approximately 1.2 Å in each cycle.[149] The film layer was around ~6 nm after 50 cycles. This should not have a big impact on the structure of the pores because their limiting dimension is about 50 nm.[157] The original pores could still be seen in the FESEM picture in Fig. 14(b), but in Fig. 14(c), the pores disappeared after 100 ALD cycles.

The ability of Al_2O_3 ALD-coated separators to cycle nano-Li_4TiO_{12} (anode (LTO))/$LiFePO_4$ (cathode (LFP)) complete cells in the range of 1.0–2.5 V at the environment temperature shows their electrochemical performance. Fig. 14(d) and (e) show the performance of the cells with a highly polar electrolyte (1 M $LiPF_6$ in pure PC). Reversible cycling was not achieved when this polar electrolyte was used in the cell with a bare separator (not illustrated). Nonetheless, the cell with the separator coated in 50 cycles utilising $LiPF_6$ in PC (Fig. 14(d)) demonstrated a nearly identical high-rate performance to the cell containing a separator without coating and traditional electrolyte, (1 M $LiPF_6$ EC/DEC) Fig. 14(d)). Additionally, after 1000 charge–discharge cycles, the cell with a 50 ALD cycle coating employing $LiPF_6$ in pure PC showed respectable cycling stability (~80% capacity retention) at 4C (Fig. 14(e)). Together, our findings demonstrate that the wetting problems were resolved and high ion conductivity was preserved when Al_2O_3 ALD-coated separators were used (see Fig. 7(e)). This can lead to an extraordinary expansion of the options as electrolyte systems. Too-narrow pores and

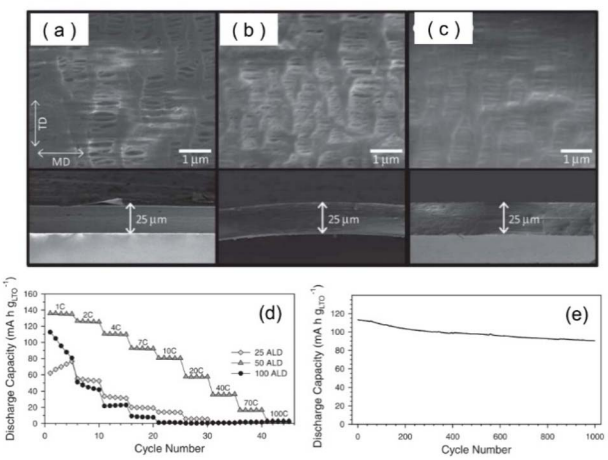

Fig. 14 Top (upper) and bottom (cross-section) FESEM images of (a) bar separators and separators coated with Al_2O_3 in (b) 50 and (c) 100 cycles. (a) Shows the transverse direction (TD) and machine direction (MD). LTO/LFP full cell electrochemical performance in 1 M $LiPF_6$ in pure propylene carbonate, utilising separators coated with Al_2O_3 by ALD (d) and (e). After 25, 50, and 100 ALD cycles, cycling data with various rates using separators coated with Al_2O_3 is shown in (d). After 50 cycles, cycle performance using a separator covered with Al_2O_3 is shown in (e). From 1.0 to 2.5 V, the cells were cycled at 4C (reprinted with permission from ref. 157 Copyright 2012 WILEY-VCH Verlag GmbH & Co. KGaA, Weinheim).

insufficient hydrophilicity are the reasons for the inferior cycling performance at various rates with the separators coated in 25 and 100 cycles employing $LiPF_6$ in PC (Fig. 14(a)). Therefore, in a polar electrolyte, 50 cycles are ideal for coating the polypropylene separator without sacrificing the high-rate capability. There are no reports on the use of pure PC as the electrolyte in polymer-based separators. It is still unclear how highly polar electrolytes completely wet the sandwiched polymer layer, despite the fact that the inorganic layers of a inorganic–polymer–inorganic trilayer separator could support the transportation and absorbing of the polar electrolyte.

When polymers are functionalized as battery separators, they should be capable of ionic transport between the positive and negative electrodes. Thus, microporous polyethylene and polyethylene are frequently used in lithium-ion batteries, which usually have a porosity of 40%.[111,173] In addition, the separators should be wetted rapidly and fully in the common battery electrolytes. In association with this requirement through the ALD process for increasing the performance of lithium-ion batteries, it has been proven that the deposition of Al_2O_3 and TiO_2 materials *via* ALD on these polymer separators may boost their wettability, which can elevate the battery performance. However, the number of ALD cycles of these materials should be considered to achieve the optimal thickness.[153] This is because an excessive thickness leads to the creation of too-narrow pores or even blocks the separator pores, which can reduce the ionic transportation through the separator membrane, which will eventually have a counter-productive effect, decreasing the battery performance.

Conclusions and outlook

ALD has shown significant promise as a flexible fabrication method for creating battery components with improved functionality. Some of the unique properties of ALD that can be a breakthrough in the endeavour to greatly improve the performance of energy storage devices include its unparalleled capabilities in terms of conformal deposition on the surface of complex structures, uniformity with pinhole-free coating, precision sub-nanometer thickness control level, and low temperature processing. Regarding the investigation to improve the battery performance, the present polymer material participation allows the extension of these advantageous properties. Given that polymers are made up of numerous units that microscopically consist of networks of polymer chains, they can be considered ideal substrates for ALD processing because they provide the two essential components needed for initial ALD growth, as follows: (i) surface groups that are reactive, such as hydroxyl groups and (ii) the space-free volume of naturally occurring polymeric chains. In general, it can be inferred from the conditions of these substrates that two different polymer growth mechanisms can occur, as follows: (i) direct growth on polymer surfaces with abundant –OH functional groups and (ii) diffusion growth for polymer surfaces without reactive sites. Owing to the ability of ALD materials to be deposited at low processing temperatures and the typically low melting temperature of polymers, the involvement of polymer materials in the ALD process can be considered a mutually beneficial relationship for the advancement of lithium-ion batteries.

The participation of polymers in the investigation of ALD material applications may be crucial to making advances in materials engineering that address a variety of problems, including the issue of energy storage. It has been demonstrated that ALD of Al_2O_3 and TiO_2 on polymers increases their wettability, which may be beneficial for battery separator applications. Regarding ionic mobility, ceramic nanocoatings (*e.g.* TiO_2) significantly decrease the resistance to ionic diffusion across porous polymeric separators. Meanwhile, the enhanced electrolyte wettability of ceramic coatings lead to a greater flow of Li^+ ions through porous separators, which in turn produces higher ionic conductivity. This is because the electrochemical performance of batteries is directly impacted by the easy movement of lithium ions between the anode and cathode, which is facilitated by a well-wettable separator. The use of ALD materials in LiB separators suggests that they can enhance the mechanical characteristics of the separator, enhance its performance in terms of safety, and eventually prevent a short-circuit between the anode and cathode, thereby reducing the risk of battery burn. Additionally, during high-temperature cycling, the performance of LiBs was improved by TiO_2-coated PE separators. The aforementioned phenomena may indicate that the coupling of the ALD method with polymer materials will be more crucial in the endeavour to develop high-performance lithium-ion batteries. Given that the mutually beneficial characteristics of polymers and the ALD process, their use in the development of lithium-ion batteries will continue to be crucial.

Data availability

No primary research results have been included as part of this review.

Conflicts of interest

There are no conflicts to declare.

Acknowledgements

This work was supported by National Research and Innovation Agency of the Republic of Indonesia (No. 196/I/KP/2025).

References

1 D. Sibanda, S. T. Oyinbo and T.-C. Jen, *Nanotechnol. Rev.*, 2022, **11**, 1332–1363.
2 T. B. Tai, J. Son and H. Shin, *Appl. Surf. Sci.*, 2023, **612**, 155702.
3 M. A. Hossain, K. Khoo, X. Cui, G. K. Poduval, T. Zhang, X. Li, W. M. Li and B. Hoex, *Nano Mater. Sci.*, 2020, **2**, 204–226.
4 Q. Peng, J. S. Lewis, P. G. Hoertz, J. T. Glass and G. N. Parsons, *J. Vac. Sci. Technol., A*, 2012, **30**, 010801–010814.

5 W. J. Sweet, C. J. Oldham and G. N. Parsons, *ACS Appl. Mater. Interfaces*, 2014, **6**, 9280–9289.
6 O. Graniel, M. Weber, S. Balme, P. Miele and M. Bechelany, *Biosens. Bioelectron.*, 2018, **122**, 147–159.
7 M. Mattinen, M. Leskelä and M. Ritala, *Adv. Mater. Interfaces*, 2021, **8**, 2001677.
8 Q. Hu, J. Xu, D. Zhang, S. Sun and G. Zhang, *Curr. Opin. Environ. Sci. Health*, 2023, **36**, 100517.
9 H. Xu, M. K. Akbari, S. Kumar, F. Verpoort and S. Zhuiykov, *Sens. Actuators, B*, 2021, **331**, 129403.
10 M. A. Güngör, O. Alev, H. K. Kaya, L. C. Arslan, S. Büyükköse, Z. Z. Öztürk and F. Kuralay, *Mater. Today Commun.*, 2023, **36**, 106776.
11 G. K. Hyde, G. Scarel, J. C. Spagnola, Q. Peng, K. Lee, B. Gong, K. G. Roberts, K. M. Roth, C. A. Hanson, C. K. Devine, S. M. Steward, D. Hojo, J.-S. Na, J. S. Jur and G. N. Parsons, *Langmuir*, 2010, **26**, 2550–2558.
12 G. N. Parsons, S. E. Atanasov, E. C. Dandley, C. K. Devine, B. Gong, J. S. Jur, K. Lee, C. J. Oldham, Q. Peng, J. C. Spagnola and P. S. Williams, *Coord. Chem. Rev.*, 2013, **257**, 3323–3331.
13 Z. Zhou, L. Xu, Y. Ding, H. Xiao, Q. Shi, X. Li, A. Li and G. Fang, *Prog. Mater. Sci.*, 2023, **138**, 101159.
14 J. Lu, *Catal. Lett.*, 2021, **151**, 1535–1545.
15 P. Kodithuwakku, D. R. Jayasundara, I. Munaweera, R. Jayasinghe, T. Thoradeniya, M. Weerasekara, P. M. Ajayan and N. Kottegoda, *Prog. Solid State Chem.*, 2022, **67**, 100369.
16 S. H. Astaneh, L. P. Faverani, C. Sukotjo and C. G. Takoudis, *Acta Biomater.*, 2021, **121**, 103–118.
17 H. Yuan, Q. Li, W. Yan, Y. Zhang, L. Chen, P. Pan, J. Luo, B. Liao and X. Ouyang, *Vacuum*, 2022, **196**, 110741.
18 T. Sheng, H. Chen, S. Xiong, X. Chen and Y. Wang, *AlChE J.*, 2014, **60**, 3614–3622.
19 M. Park, S. Oh, H. Kim, D. Jung, D. Choi and J.-S. Park, *Thin Solid Films*, 2013, **546**, 153–156.
20 H. Shin, D.-K. Jeong, J. Lee, M. M. Sung and J. Kim, *Adv. Mater.*, 2004, **16**, 1197–1200.
21 J. S. King, E. Graugnard, O. M. Roche, D. N. Sharp, J. Scrimgeur, R. G. Denning, A. J. Turberfield and C. J. Summers, *Adv. Mater.*, 2006, **18**, 1561–1565.
22 B. Gong, Q. Peng, J. S. Jur, C. K. Devine, K. Lee and G. N. Parsons, *Chem. Mater.*, 2011, **23**, 3476–3485.
23 X. Meng, *Nanotechnology*, 2015, **26**, 020501.
24 X. Meng, X.-Q. Yang and X. Sun, *Adv. Mater.*, 2012, **24**, 3589–3615.
25 X. Meng, X. Wang, D. Geng, C. Ozgit-Akgun, N. Schneider and J. W. Elam, *Mater. Horiz.*, 2017, **4**, 133–154.
26 E. Riyanto, E. Martides, G. Pikra, T. D. Atmaja, R. I. Pramana, A. J. Purwanto, A. Santosa, E. Junianto, R. Darussalam, A. Saepudin, A. Susatyo, R. A. Subekti, Y. S. Utomo, D. G. Subagio, A. Fudholi, H. Abimanyu, Y. Radiansah, H. Sudibyo, K. Kusnadi, A. Rajani, S. Suprapto and B. Prawara, *J. Mater. Res. Technol.*, 2021, **15**, 5466–5481.
27 H. Xu, M. K. Akbari and S. Zhuiykov, *Nanoscale Res. Lett.*, 2021, **16**, 1–38.
28 M. Leskelä and M. Ritala, *Angew. Chem., Int. Ed.*, 2003, **42**, 5548–5554.
29 D. Escorcia-Díaz, S. García-Mora, L. Rendón-Castrillón, M. Ramírez-Carmona and C. Ocampo-López, *Nanomaterials*, 2023, **13**, 2586.
30 N. Pastukhova, A. Mavrič and Y. Li, *Adv. Mater. Interfaces*, 2021, **2002100**, 1–22.
31 A. U. Mane, W. M. Tong, A. D. Brodie, M. A. McCord and J. W. Elam, *ECS Trans.*, 2014, **64**, 3–14.
32 X. Wang, *Chem. Mater.*, 2021, **33**, 6251–6268.
33 R. L. Puurunen, *J. Appl. Phys.*, 2005, **97**, 121301.
34 N. Biyikli and A. Haidar, *Semicond. Sci. Technol.*, 2017, **32**, 093002.
35 S. Kim, S. Lee, S.-Y. Ham, D.-H. Ko, S. Shin and Z. Jin, *Appl. Surf. Sci.*, 2019, **469**, 804–810.
36 J. A. Oke and T.-C. Jen, *J. Mater. Res. Technol.*, 2022, **21**, 2481–2514.
37 T. Nam and H. Kim, *J. Mater. Res.*, 2020, **35**, 656–680.
38 O. Y. Ramírez-Esquivel, D. A. Mazón-Montijo, D. Cabrera-German, E. Martínez-Guerra and Z. Montiel-González, *Ceram. Int.*, 2021, **47**, 7126–7134.
39 Y. Zhou, J. Wang, P. He, S. Chen, Z. Chen, Y. Zang, Y. Li and Y. Duan, *J. Electron. Mater.*, 2022, **51**, 2766–2785.
40 J. Baek, K. Nam, J.-y. Park and J. Cha, *Appl. Surf. Sci.*, 2022, **606**, 154695.
41 H. Kim, *Thin Solid Films*, 2011, **519**, 6639–6644.
42 J. S. Ponraj, G. Attolini and M. Bosi, *Crit. Rev. Solid State Mater. Sci.*, 2013, **38**, 203–233.
43 R. L. Puurunen, *Appl. Surf. Sci.*, 2005, **245**, 6–10.
44 D. J. Hagen, M. E. Pemble and M. Karppinen, *Appl. Phys. Rev.*, 2019, **6**, 041309.
45 R. Cooper, H. P. Upadhyaya, T. K. Minton, M. R. Berman, X. Du and S. M. George, *Thin Solid Films*, 2008, **516**, 4036–4039.
46 C. Zhu, K. Han, D. Geng, H. Ye and X. Meng, *Electrochim. Acta*, 2017, **251**, 710–728.
47 G. K. Hyde, S. D. McCullen, S. Jeon, S. M. Stewart, H. Jeon, E. G. Loboaand and N. Parsons, *Biomed. Mater.*, 2009, **4**, 025001.
48 X. Jia, Z. Low, H. Chen, S. Xiong and Y. Wang, *Chin. J. Chem. Eng.*, 2018, **26**, 695–700.
49 G. Song and D. Q. Tan, *Macromol. Mater. Eng.*, 2020, **2000127**, 1–24.
50 Y. Xu and C. B. Musgrave, *Chem. Mater.*, 2004, **16**, 646–653.
51 S.-Y. Ham, Z. Jin, S. Shin, M. Kim, M. Seo and Y.-S. Min, *Appl. Surf. Sci.*, 2022, **571**, 151282.
52 J. I. Paez-Ornelas, H. N. Fernandez-Escamilla, H. A. Borbon-Nunez, H. Tiznado, N. Takeuchi and J. Guerrero-Sanchez, *Phys. Chem. Chem. Phys.*, 2021, **23**, 3467–3478.
53 V. Cremers, R. L. Purunen and J. Dendooven, *Appl. Phys. Rev.*, 2019, **6**, 021302.
54 J. A. Oke and T.-C. Jen, *Int. J. Adv. Manuf. Technol.*, 2023, **126**, 4811–4825.
55 K. K. Mentel, A. V. Emelianov, A. Philip, A. Johansson, M. Karppinen and M. Pettersson, *Adv. Mater. Interfaces*, 2022, **9**, 2201110.
56 Y. K. Lee, C. Yoo, W. Kim, J. W. Jeona and C. S. Hwang, *J. Mater. Chem. C*, 2021, **9**, 3708–3725.

57 H. Liu, P. Ma, Y. Pu and Z. Zhao, *J. Alloys Compd.*, 2021, **859**, 157751.
58 A. A. Barmpaki, E. E. Zavvou, C. Drivas, K. Papapetros, L. Sygellou, N. D. Andritsos, A. Giannakas, C. E. Salmas, A. Ladavos, P. Svarnas, P. K. Karahaliou and C. A. Krontiras, *J. Appl. Polym. Sci.*, 2023, **140**, 54465.
59 M. O. Faruk, A. Ahmed, M. A. Jalil, M. T. Islam, A. M. Shamim, B. Adak, M. M. Hossain and S. Mukhopadhyay, *Appl. Mater. Today*, 2021, **23**, 101025.
60 E. Riyanto, E. Martides, E. Junianto and B. Prawara, *Eksergi*, 2020, **17**, 56–61.
61 K. K. Chawla, *Fibrous Materials*, Cambridge University Press, Cambridge, United Kingdom, 1998.
62 I. E. Kelly, J. R. Owen and B. C. H. Steele, *J. Power Sources*, 1985, **14**, 13–21.
63 R. Kaindl, T. Homola, A. Rastelli, A. Schwarz, A. Tarre, D. Kopp, A. M. Coclite, M. Götler, B. Meier, B. Prettenthaler, M. Belegratis, J. M. Lackner and W. Waldhauser, *Surf. Interfaces*, 2022, **34**, 102361.
64 J.-M. Tarascon and M. Armand, *Nature*, 2001, **414**, 359–367.
65 Y. Chen, Y. Kang, Y. Zhao, L. Wang, J. Liu, Y. Li, Z. Liang, X. He, X. Li, N. Tavajohi and B. Li, *J. Energy Chem.*, 2021, **59**, 83–99.
66 A. Ershad-Langroudi, N. Babazadeh, F. Alizadegan, S. M. Mousaei and G. Moradi, *J. Ind. Eng. Chem.*, 2024, **137**, 61–86.
67 J. He, Z. Liu, W. Zhang, C. He and W. Li, *Surf. Interfaces*, 2023, **42**, 103477.
68 R. Edy, Y. T. Zhao, G. S. Huang, J. J. Shi, J. Zhang, A. A. Solovev and Y. F. Mei, *Prog. Nat. Sci.: Mater. Int.*, 2016, **26**, 493–497.
69 R. Edy, *Two-dimensional Material Fabricated by Atomic Layer Deposition for Photocatalysis*, PhD Thesis, Donghua University, 2017.
70 K. Lee, D. H. Kim and G. N. Parsons, *ACS Appl. Mater. Interfaces*, 2014, **6**, 10981–10985.
71 R. E. Shallman and R. J. Bishop, *Modern Physical Metallurgy & Materials Engineering*, Elsevier Science Ltd, London, England, 1999.
72 W. D. C. Jr and D. G. Rethwisch, *Fundamentals of Materials Science and Engineering: an Integrated Approach*, John Wiley & Sons, Inc, United States, 2008.
73 M. A. Shah, B. M. Pirzada, G. Price, A. L. Shibiru and A. Qurashi, *J. Adv. Res.*, 2022, **38**, 55–75.
74 Q. Shi, J. Sun, C. Hou, Y. Li, Q. Zhang and H. Wang, *Adv. Fiber Mater.*, 2019, **1**, 3–31.
75 A. Khan, M. N. Haque, D. C. Kabiraz, A. Yeasin, H. A. Rashid, A. C. Sarker and G. Hossain, *Sens. Actuators, A*, 2023, **350**, 114093.
76 M.-R. Azani and A. Hassanpour, *J. Mater. Sci.: Mater. Electron.*, 2024, **35**, 1897.
77 J. S. Meena, S. B. Choi, S.-B. Jung and J.-W. Kim, *Mater. Today Bio*, 2023, **19**, 100565.
78 A. H. Brozena, C. J. Oldham and G. N. Parsons, *J. Vac. Sci. Technol., A*, 2015, **34**, 010801–010817.
79 I. Marriam, X. Wang, M. Tebyetekerwa, G. Chen, F. Zabihi, J. Pionteck, S. Peng, S. Ramakrishna, S. Yang and M. Zhu, *J. Mater. Chem. A*, 2018, **6**, 13633–13643.
80 M.-Y. Liu, Y.-F. Zhang, L.-X. Ou, L.-Y. Zhu, X.-Y. Wu, Y. Wang, Y. Gu, Y.-C. Chen and H.-L. Lu, *Appl. Mater. Today*, 2024, **37**, 102099.
81 H. Chen, S. Wu, X. Jia, S. Xiong and Y. Wang, *Am. Inst. Chem. Eng. J.*, 2018, **64**, 2670–2678.
82 C. Kun, L. Xiao, Y. Fan and C. Rong, *Sci. China: Technol. Sci.*, 2022, **65**, 2218–2220.
83 G. Marin, R. Funahashi and M. Karpinen, *Adv. Eng. Mater.*, 2020, **22**, 2000535.
84 M. N. Badawi, N. Agrawal, S. F. Adil, S. Ramesh, K. Ramesh and S. Bashir, *New Carbon Mater.*, 2023, **38**, 211–229.
85 J. Jiang, X. Chen, Y. Niu, X.-r. He, Y.-l. Hu and C. Wang, *New Carbon Mater.*, 2022, **37**, 303–320.
86 J. Feng, S. Xiong, Z. Wang, Z. Cui, S.-P. Sun and Y. Wang, *J. Membr. Sci.*, 2018, **550**, 246–253.
87 S. M. George, *Chem. Rev.*, 2010, **110**, 111–131.
88 W. M. M. E. Kessels and M. Putkonen, *MRS Bull.*, 2011, **36**, 907–913.
89 M. Coll and M. Napari, *APL Mater.*, 2019, **7**, 110901.
90 M. Napari, J. Malm, R. Lehto, J. Julin, K. Arstila, T. Sajavaara and M. Lahtinen, *J. Vac. Sci. Technol., A*, 2015, **33**, 01A128.
91 J. S. Jur, J. C. Spagnola, K. Lee, B. Gong, Q. Peng and G. N. Parsons, *Langmuir*, 2010, **26**, 8239–8244.
92 H.-S. Cho, N. Shin, K. Kim, B. Kim and D.-H. Kim, *Synth. Met.*, 2015, **207**, 31–34.
93 J. W. Elam, N. P. Dasgupta and F. B. Prinz, *MRS Bull.*, 2011, **36**, 899–906.
94 K. Gregorczyk and M. Knez, *Prog. Mater. Sci.*, 2016, **75**, 1–37.
95 K. Sharma, D. Routkevitch, N. Varaksa and S. M. George, *J. Vac. Sci. Technol., A*, 2016, **34**, 01A146.
96 T. Ahmadzada, D. R. Mckenzie, N. L. James, Y. Yin and Q. Li, *Thin Solid Films*, 2015, **591**, 131–136.
97 Z. Giedraityte, P. Sundberg and M. Karppinen, *J. Mater. Chem. C*, 2015, **3**, 12316.
98 M. D. Groner, F. H. Fabreguette, J. W. Elam and S. M. George, *Chem. Mater.*, 2004, **16**, 639–645.
99 A. Bulusu, A. Singh, C. Y. Wang, A. Dindar, C. Fuentes-Hernandez, H. Kim, D. Cullen, B. Kippelen and S. Graham, *J. Appl. Phys.*, 2015, **118**, 085501.
100 W. Xiao, D. Y. Hui, C. Zheng, D. Yu, Y. Y. Qiang, C. Ping, C. L. Xiang and Z. Yi, *Nanoscale Res. Lett.*, 2015, **10**, 130.
101 P. S. Maydannik, A. Plyushch and M. Sillanpää, *J. Vac. Sci. Technol., A*, 2015, **33**, 031603.
102 H. Klumbies, P. Schmidt, M. Hähnel, A. Singh, U. Schroeder, C. Richter, T. Mikolajick, C. Hoßbach, M. Albert, J. W. Bartha, K. Leo and L. Müller-Meskamp, *Org. Electron.*, 2015, **17**, 138–143.
103 T. Hirvikorpi, R. Laine, M. Vähä-Nissi, V. Kilpi, E. Salo, W.-M. Li, S. Linfors, J. Vartiainen, E. Kenttä, J. Nikkola, A. Harlin and J. Kostamo, *Thin Solid Films*, 2014, **550**, 164–169.
104 K. Ali, K.-H. Choi, J. Jo and Y. W. Lee, *Mater. Lett.*, 2014, **136**, 90–94.
105 J. Ahn, C. Ahn, S. Jeon and J. Park, *Appl. Sci.*, 2019, **9**, 1990.
106 H. Kim, H.-B.-R. Lee and W.-J. Maeng, *Thin Solid Films*, 2009, **517**, 2563–2580.

107 T. Hirvikorpi, M. V. -Nissi, A. Harlin, J. Marles, V. Miikkulainen and M. Karppinen, *Appl. Surf. Sci.*, 2010, **257**, 736–740.
108 S. Gieraltowska, L. Wachnicki, B. S. Witkowski, R. Mroczynski, P. Dluzewski and M. Godlewski, *Thin Solid Films*, 2015, **577**, 97–102.
109 J. G. Lee, H. G. Kim and S. S. Kim, *Thin Solid Films*, 2015, **577**, 143–148.
110 A. D. Mauro, M. Cantarella, G. Nicotra, V. Privitera and G. Impellizzeri, *Appl. Catal., B*, 2016, **196**, 68–76.
111 C.-H. Chao, C.-T. Hsieh, W.-J. Ke, L.-W. Lee, Y.-F. Lin, H.-W. Liu, S. Gu, C.-C. Fu, R.-S. Juang, B. C. Mallick, Y. A. Gandomi and C.-Y. Su, *J. Power Sources*, 2021, **482**, 228896.
112 L. Nyholmm, G. Nyström, A. Mihranyan and M. Strømme, *Adv. Mater.*, 2011, **23**, 3151–3769.
113 R. J. Narayan, S. P. Adiga, M. J. Pellin, L. A. Curtiss, A. J. Hryn, S. Stafslien, B. Chisholm, C.-C. Shih, C.-M. Shih, S.-J. Lin, Y.-Y. Su, C. Jin, J. Zhang, N. A. Monteiro-Riviere and J. W. Elam, *Philos. Trans. R. Soc., A*, 2010, **368**, 2033–2064.
114 A. W. Ott, J. W. Klaus, J. M. Johnson and S. M. George, *Thin Solid Films*, 1997, **292**, 135–144.
115 J. Gong, S. Shi, S. Cheng, K. Yang, P. Zheng, Y. Xu, J. Chai, Y. Zheng, Z. Liu and M. Xie, *Appl. Surf. Sci.*, 2024, **659**, 159918.
116 S. Ng, C. Iffelsberger, J. Michalička and M. Pumera, *ACS Nano*, 2021, **15**, 686–697.
117 E. Riyanto, D. Dedi, A. Fudholi, G. Ying, Z. Jing, S. Jianjun, H. Gaoshan and M. Yongfeng, *Mater. Res. Express*, 2023, **10**, 096401.
118 R. Edy, X. J. Huang, Y. Guo, J. Zhang and J. J. Shi, *Nanoscale Res. Lett.*, 2013, **8**(79), 1–9.
119 R. Edy, G. S. Huang, Y. T. Zhao, Y. Guo, J. Zhang, Y. F. Mei and J. J. Shi, *Surf. Coat. Technol.*, 2017, **329**, 149–154.
120 M. B. M. Mousa, J. S. Ovental, A. H. Brozena, C. J. Oldham and G. N. Parsons, *J. Vac. Sci. Technol., A*, 2018, **36**, 031517.
121 C. X. Wang, M. Du and Y. Qiu, *Surf. Coat. Technol.*, 2010, **205**, 3575–3580.
122 R. Morent, N. D. Geyter, J. Verschuren, K. D. Clerck, P. Kiekens and C. Leys, *Surf. Coat. Technol.*, 2008, **202**, 3427–3449.
123 S. M. Goerge, *Chem. Rev.*, 2010, **110**, 111–131.
124 R. L. Puurunen, A. Root, P. Sarv, M. M. Viitanen, H. H. Brongersma, M. Lindblad and A. O. I. Krause, *Chem. Mater.*, 2002, **14**, 720–729.
125 Q. Xie, Y.-L. Jiang, C. Detavernier, D. Deduytsche, R. L. V. Meirhaeghe, G.-P. Ru, B.-Z. Li and X.-P. Qu, *J. Appl. Phys.*, 2007, **102**, 083521.
126 F. Zaera, *Coord. Chem. Rev.*, 2013, **257**, 3177–3191.
127 Z. Xiao, K. Kisslinger and R. Monikandan, *J. Carbon Res.*, 2021, **7**, 67.
128 N. Gong, H. Seet, J. Cao, T. L. Meng, Y. Wang, D. C. C. Tan, C. K. I. Tan, A. Suwardi, Q. Zhu, D. J. Blackwood, M. L. S. Nai and H. Liu, *Mater. Lett.*, 2023, **331**, 133434.
129 O. Toikkanen, M. Nisula, E. Pohjalainen, S. Hietala, H. Havansi, J. Ruotsalainen, S. Halttunen, M. Karppinen and T. Kallio, *J. Membr. Sci.*, 2015, **495**, 101–109.
130 A. Nourbakhsh, C. Adelmann, Y. Song, C. S. Lee, I. Asselberghs, C. Huyghebaert, S. Brizzi, M. Tallarida, D. Schmeißer, S. V. Elshocht, M. Heyns, J. Kong, T. Palacios and S. D. Gendt, *Nanoscale*, 2015, **7**, 10781–10789.
131 J. S. Jur, J. C. Spagnola, K. Lee, B. Gong and G. N. Parsons, *Langmuir*, 2010, **26**, 8239–8244.
132 T. Hirvikorpi, M. V. -Nissi, J. Nikkola, A. Harlin and M. Karppinen, *Surf. Coat. Technol.*, 2011, **205**, 5088–5092.
133 Q. Peng, X.-Y. Sun, J. C. Spagnola, G. K. Hyde, R. J. Spontak and G. N. Parsons, *Nano Lett.*, 2007, **7**, 719–722.
134 C. Detavernier, J. Dendooven, S. P. Sree, K. F. Ludwig and J. A. Martens, *Chem. Soc. Rev.*, 2011, **40**, 5242–5253.
135 H. C. Guo, E. Ye, Z. Li, M.-Y. Han and X. J. Loh, *Mater. Sci. Eng., C*, 2017, **70**, 1182–1191.
136 D. N. Goldstein, J. A. McCormick and S. M. George, *J. Phys. Chem. C*, 2008, **112**, 19530–19539.
137 J. Li, G. Chai and X. Wang, *Int. J. Extreme Manuf.*, 2023, **5**, 032003.
138 C. Argile and G. E. Rhead, *Surf. Sci. Rep.*, 1989, **10**, 277–356.
139 J. D. Ferguson, A. W. Weimer and S. M. George, *Chem. Mater.*, 2004, **16**, 5602–5609.
140 M. Kemell, E. Färm, M. Ritala and M. Leskelä, *Eur. Polym. J.*, 2008, **44**, 3564–3570.
141 M. Naguib, O. Mashtalir, J. Carle, V. Presser, J. Lu, L. Hultman, Y. Gogotsi and M. W. Barsoum, *ACS Nano*, 2012, **6**, 1322–1331.
142 T. Itzhak, N. Segev-Mark, A. Simon, V. Abetz, G. Z. Ramon and T. Segal-Peretz, *ACS Appl. Mater. Interfaces*, 2021, **13**, 15591–15600.
143 M. Weber, A. Julbe, A. Ayral, P. Miele and M. Bechelany, *Chem. Mater.*, 2018, **30**, 7368–7390.
144 S. Xiong, X. Qian, Z. Zhong and Y. Wang, *J. Membr. Sci.*, 2022, **658**, 120740.
145 E. Riyanto, *ScienceAsia*, 2020, **46**, 444–449.
146 Z. Li, J. Su and X. Wang, *Carbon*, 2021, **179**, 299–326.
147 L. Aarik, C.-T. Piller, J. Raud, R. Talviste, I. Jõgi and J. Aarik, *J. Cryst. Growth*, 2023, **609**, 127148.
148 J. Casetta, D. G. Ortiz, C. Pochat-Bohatier, M. Bechelany and P. Miele, *Sep. Purif. Technol.*, 2023, **312**, 123377.
149 C. A. Wilson, R. K. Grubbs and S. M. George, *Chem. Mater.*, 2005, **17**, 5625–5634.
150 C. Luo, H. Zhu, W. Luo, F. Shen, X. Fan, J. Dai, Y. Liang, C. Wang and L. Hu, *ACS Appl. Mater. Interfaces*, 2017, **9**, 14801–14807.
151 X. Shen, C. Li, C. Shi, C. Yang, L. Deng, W. Zhang, L. Peng, J. Dai, D. Wu, P. Zhang and J. Zhao, *Appl. Surf. Sci.*, 2018, **441**, 165–173.
152 G. D'Acunto, S. B. Shuchi, X. Zheng, L. V. Than, E. M. Geierstanger, M. Harake, A. Cui, A. Werbrouck, M. Mattinen, Y. Cui and S. F. Bent, *ACS Appl. Mater. Interfaces*, 2025, **17**, 7007–7018.
153 W. Wang, Y. Yuan, J. Wang, Y. Zhang, C. Liao, X. Mu, H. Sheng, Y. Kan, L. Song and Y. Hu, *ACS Appl. Mater. Interfaces*, 2019, **2**, 4167–4174.
154 H. Chen, Q. Lin, Q. Xu, Y. Yang, Z. Shao and Y. Wang, *J. Membr. Sci.*, 2014, **458**, 217–224.

155 Y. Zhao, G. Huang, Y. Li, R. Edy, P. Gao, H. Tang, Z. Bao and Y. Mei, *J. Mater. Chem. A*, 2018, **6**, 7227.
156 L. P. da Veiga, C. Jeanguenat, F. Lisco, H.-Y. Li, S. Nicolay, C. Ballif, A. Ingenito and J. J. D. Leon, *ACS Omega*, 2022, **7**, 45582–45589.
157 Y. S. Jung, A. S. Cavanagh, L. Gedvilas, N. E. Widjonarko, I. D. Scott, S.-H. Lee, G.-H. Kim, S. M. George and A. C. Dillon, *Adv. Energy Mater.*, 2012, **2**, 1022–1027.
158 X. Sun, M. Xie, G. Wang, H. Sun, A. S. Cavanagh, J. J. Travis, S. M. George and J. Lian, *J. Electrochem. Soc.*, 2012, **159**, A364–A369.
159 S. J. A. Zaidi, J. C. Park, J. W. Han, J. H. Choi, M. A. Ali, M. A. Basit and T. J. Park, *Small Sci.*, 2023, **3**, 2300060.
160 P. Poizot, S. Laruelle, S. Grugeon, L. Dupont and J.-M. Tarascon, *Nature*, 2000, **407**, 496–499.
161 C. K. Chan, H. Peng, G. Liu, K. McIlwrath, X. F. Zhang, R. A. Huggins and Y. Cui, *Nat. Nanotechnol.*, 2008, **3**, 31–35.
162 A. Y. Galashev, K. A. Ivanichkina and O. R. Rakhmanova, *Comput. Mater. Sci.*, 2021, **200**, 110771.
163 J. Su, Z. Li, Y. Yu and X. Wang, *Adv. Mater. Interfaces*, 2017, **1600835**, 1–17.
164 Z. Han, C. Zhang, Q. Lin, Y. Zhang, Y. Deng, J. Han, D. Wu, F. Kang, Q.-H. Yang and W. Lv, *Small Methods*, 2021, **5**, 2001035.
165 D. Deng, *Energy Sci. Eng.*, 2015, **3**, 385–418.
166 M. Koo, K. I. Park, S. H. Lee, M. Suh, D. Y. Jeon, J. W. Choi, K. Kang and K. J. Lee, *Nano Lett.*, 2012, **12**, 4810–4816.
167 S.-Y. Lee, K.-H. Choi, W.-S. Choi, Y. H. Kwon, H.-R. Jung, H.-C. Shin and J. Y. Kim, *Energy Environ. Sci.*, 2013, **6**, 2414–2423.
168 Y. Hu and X. Sun, *J. Mater. Chem. A*, 2014, **2**, 10712.
169 E. Langereis, M. Creatore, S. B. S. Heil, M. C. M. v. d. Sanden and W. M. M. Kessels, *Appl. Phys. Lett.*, 2006, **89**, 081915.
170 S. H. Lim, S.-W. Seo, H. Lee, H. Chae and S. M. Cho, *Korean J. Chem. Eng.*, 2016, **33**, 1971–1976.
171 P. Johansson, H. Teisala, K. Lahtinen and J. Kuusipalo, *Thin Solid Films*, 2017, **621**, 151–155.
172 B. Padha, Z. Ahmed, S. Dutta, A. Pandey, N. Padha, M. Tomar, A. Sharma, I. Yadav and S. Arya, *J. Alloys Compd.*, 2025, **1010**, 177673.
173 P. Arora and Z. Zhang, *Chem. Rev.*, 2004, **104**, 4419–4462.
174 P. Zhai, K. Liu, Z. Wang, L. Shi and S. Yuan, *J. Power Sources*, 2021, **499**, 229973.
175 D. Linden and T. B. Reddy, *Handbook of Batteries*, The McGraw-Hill Companies, Inc., New York, 2002.
176 B. Gong and G. N. Parsons, *J. Mater. Chem.*, 2012, **22**, 15672–15682.
177 Q. Xu, J. Yang, J. Dai, Y. Yang, X. Chen and Y. Wang, *J. Membr. Sci.*, 2013, **448**, 215–222.
178 S.-i. Tobishima and J.-i. Yamaki, *J. Power Sources*, 1999, **81–82**, 882–886.
179 Y. Mao, W. Sun, Y. Qiao, X. Liu, C. Xu, L. Fang, W. Hou, Z. Wang and K. Sun, *Chem. Eng. J.*, 2021, **416**, 129119.